

Supporting Information

Metal-free Upcycling of Plastic Waste: Photo-induced Oxidative Degradation of Polystyrene in Air

Shuoyu Xu[#], Shuxin Liu[#], Wangze Song, Nan Zheng^{*}

School of Chemical Engineering, Dalian University of Technology, Linggong Rd. 2, Dalian, Liaoning 116023, China

**Corresponding author:*

N. Z. E-mail: nzheng@dlut.edu.cn

Contents

1. General information.....	4
2. Preparation of the photocatalysts.....	5
2.1 Synthesis of photocatalyst PPOP-1.....	5
2.2 Synthesis of photocatalyst PPOP-2.....	6
2.3 Synthesis of photocatalyst PPOP-3.....	6
2.4 Synthesis of photocatalyst PPOP-4.....	7
2.5 Synthesis of photocatalyst PPOP-5.....	8
2.6 Synthesis of photocatalyst PPOP-6.....	9
2.7 Synthesis of photocatalyst PPOP-7.....	10
3. Analysis and characterization of photocatalyst PPOP-1.....	12
3.1 Fourier-transformed infrared spectrum of photocatalyst PPOP-1.....	12
3.2 SEM image of photocatalyst PPOP-1.....	13
3.3 BET surface areas of photocatalyst PPOP-1.....	13
3.4 UV-vis spectrum of photocatalyst PPOP-1.....	14
3.5 X-ray diffraction patterns of photocatalyst PPOP-1.....	14
3.6 Thermogravimetric analysis image of photocatalyst PPOP-1.....	15
4. Details of photoreactor.....	16
5. Optimization of reaction conditions.....	17
6. Analysis and characterization of photocatalyst PPOP-7.....	22
6.1 UV-vis spectra of 1 and 8.....	22
6.2 Fourier-transformed infrared spectrum of photocatalyst PPOP-7.....	23
6.3 SEM image of photocatalyst PPOP-7.....	23
6.4 BET surface areas of photocatalyst PPOP-7.....	24
6.5 UV-vis spectrum of photocatalyst PPOP-7.....	24
6.6 X-ray diffraction patterns of photocatalyst PPOP-7.....	25
6.7 Thermogravimetric analysis image of photocatalyst PPOP-7.....	25
7. Aerobic degradation of different types of polymers.....	26
7.1 Aerobic degradation of PS.....	26
7.2 Aerobic degradation of HIPS.....	27
7.3 Aerobic degradation of SAN.....	27
7.4 Aerobic degradation of ABS.....	28
7.5 Aerobic degradation of polymer waste from our daily life.....	28
8. Characterization of PS degradation.....	31
8.1 Water contact angle measurement.....	31

8.2 X-Ray Diffraction	31
8.3 Glass transition temperature	32
8.4 GPC experiments	33
9. ICP-MS determined possible metal residues of photocatalysts PPOP-1 and PPOP-7	34
9.1 ICP-MS determined possible metal residues of photocatalyst PPOP-1	34
9.2 ICP-MS determined possible metal residues of photocatalyst PPOP-7	34
10. Comparison of reactive oxygen species yield of TPP, PPOP-1 and PPOP-7	35
11. UV-vis spectra of photocatalysts PPOP-2, PPOP-3, PPOP-4, PPOP-5 and PPOP-6	36
12. UV-vis spectra of photocatalyst PPOP-7 at different times of reaction	37
13. Control experiments.....	38
14. Characterization data	40
15. References.....	43
16. Copies of NMR Spectra of Products.....	44

1. General information

Unless otherwise noted, all commercially available reagents and solvents were used without further purification. All plastics (polystyrene: PS; high impact resistant polystyrene: HIPS; styrene-acrylonitrile: SAN; acrylonitrile-butadiene-styrene: ABS) are commercially available unless otherwise noted. Thin layer chromatography was performed using precoated silica gel plates and visualized with UV light at 254 nm. Flash column chromatography was performed with silica gel (40-60 μm). The photocatalytic reactions were performed on WATTCAS Parallel Light Reactor (WP-TEC-1020HSL). ^1H NMR spectra and ^{13}C NMR spectra were recorded on Bruker AVANCE II 400 NMR spectrometer, Vaian DLG 400MHz and Bruker Avance NEO 600M NMR Spectroscopy. Signal splitting patterns were described as singlet (s), doublet (d), triplet(t), quartet (q), quintet (quint), or multiplet (m), with coupling constants (J) in hertz (Hz). High resolution mass spectra (HRMS) were performed by an Agilent apparatus (TOF mass analyzer type) on an Electron Spray Injection (ESI) mass spectrometer. Scanning electron microscopy (SEM) was performed on NOVA NanoSEM 450 (FEI). Fourier Transform Infrared Spectrometer (FT-IR) was performed on Thermo Scientific Nicolet 6700. Physical adsorption was performed on AUTO SORB-1-MP. The inductively coupled plasma-mass spectrometry (ICP-MS) was recorded by ICP-MS-7700. The number-average molecular weight (M_n), weight-average molecular weight (M_w) and polydispersity index (PDI) of polymers were determined by gel permeation chromatography (GPC) equipped with an isocratic pump (model 1515, Waters Corporation) (mobile phase: DMF; standard: polystyrene). The UV-vis spectra (UV-vis) were measured on Lambda 1050+. X-ray diffraction patterns were measured on Bruker D8 Advance. TGA images were obtained with Q-500. The glass transition temperature obtained by Q2000. The water contact angle measured by JCD2000D2W. The fluorescence intensity (at 500-700 nm) was measured using the multifunctional enzyme marker Synergy H1 (BioTek, USA).

The yield formula is the amount of benzoic acid produced divided by the amount of benzene rings contained in the PS reactant. The formula for selectivity is the amount of benzoic acid produced divided by the total amount of all benzene ring-containing organics produced (i.e., benzoic acid and acetophenone). The two formulas are as follows:

$$\text{yield} = \frac{\text{the amount of benzoic acid produced}}{\text{the amount of benzene rings contained in the PS reactant}}$$

$$\text{selectivity} = \frac{\text{the amount of benzoic acid produced}}{\text{the total amount of benzoic acid and acetophenone produced}}$$

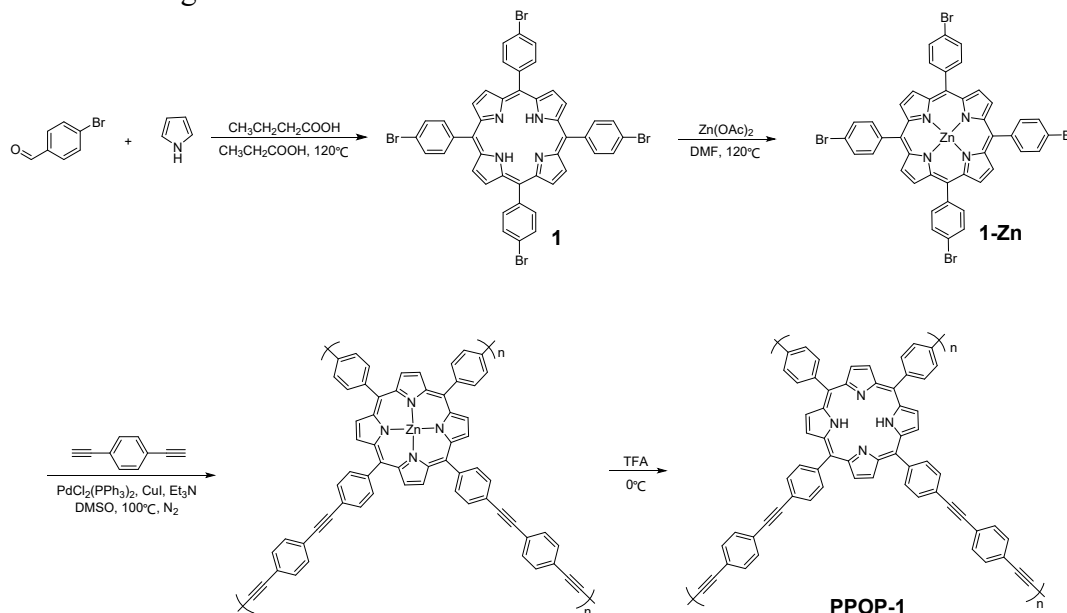
2. Preparation of the photocatalysts

The insoluble photocatalyst was synthesized by polymerization of porphyrin monomer *via* a Sonogashira polycondensation reaction, resulting in insoluble porphyrin-based porous organic polymers (**PPOPs**) (**PPOP-1 to PPOP-7 corresponds with Scheme S1 to S7**). Owing to highly cross-linked network structures, **PPOPs** were insoluble in almost all organic and inorganic solvents including CH_2Cl_2 , acetone, MeOH, THF, DMF, DMSO, MeCN, toluene and H_2O .

2.1 Synthesis of photocatalyst PPOP-1

According to reported synthetic methods,^{S1} pyrrole (2 mL, 30 mmol) and 4-bromobenzaldehyde (5 g, 30 mmol) were dissolved in the mixture of propionic acid (45 mL) containing acetic acid (15 mL), followed by stirred at 120 °C for 2 h. After cooling to room temperature, it was washed with formic acid and dried to obtain 5,10,15,20-tetrakis(4-bromophenyl)-porphyrin (**1**) (5.65 g, 90%). To a solution of **1** (280 mg, 0.3 mmol) in DMF (3 mL), anhydrous zinc acetate (275 mg, 1.5 mmol) was added and stirred at 120 °C for 3 h. The red zinc porphyrin complex Zn(II)(5,10,15,20-tetrakis(4-bromophenyl)-porphyrin) (**1-Zn**) (268 mg, 90%) was obtained after being washed with deionized water and dried.

To a solution of **1-Zn** (150 mg, 0.15 mmol), 1,4-diethynylbenzene (38 mg, 0.3 mmol), $\text{PdCl}_2(\text{PPh}_3)_2$ (42 mg, 0.06 mmol) and CuI (5.7 mg, 0.03 mmol) in DMSO (2 mL), TEA (1 mL) was added and the mixture was stirred at 100 °C for 30 min. The product was precipitated using CH_2Cl_2 and collected by centrifugation, which was further soaked with TFA to remove zinc. Red insoluble porphyrin-based porous organic polymer (**PPOP-1**) (117 mg, 85%) was obtained after being washed with deionized water and dried.

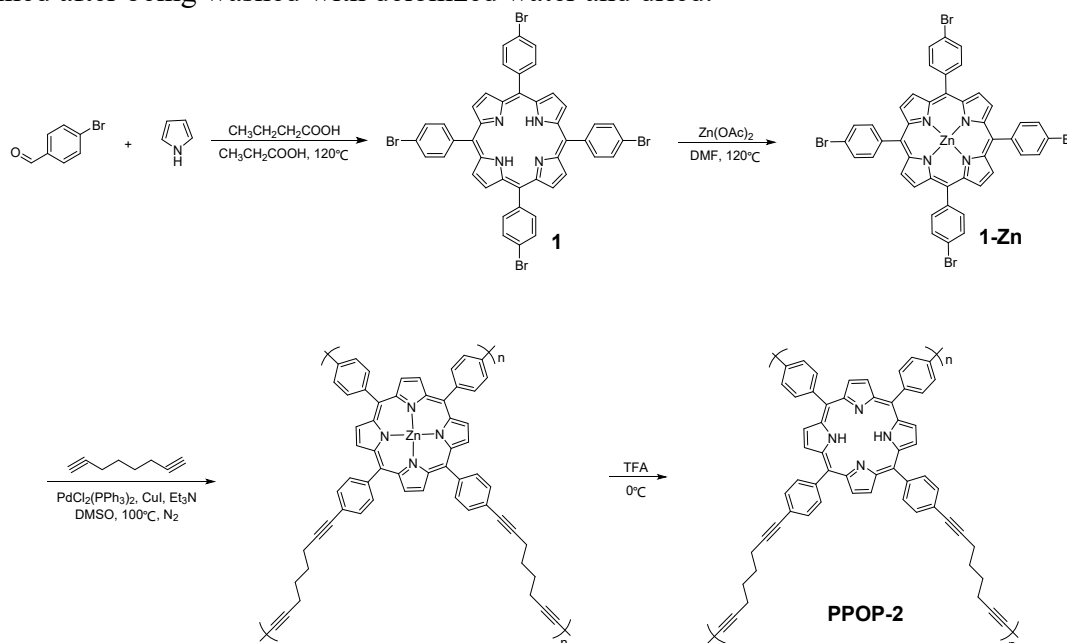


Scheme S1. Synthesis of photocatalyst PPOP-1

2.2 Synthesis of photocatalyst PPOP-2

Pyrrole (2 mL, 30 mmol) and 4-bromobenzaldehyde (5 g, 30 mmol) were dissolved in the mixture of propionic acid (45 mL) containing acetic acid (15 mL), followed by stirred at 120 °C for 2 h. After cooling to room temperature, it was washed with formic acid and dried to obtain 5,10,15,20-tetrakis(4-bromophenyl)-porphyrin (**1**) (5.65 g, 90%). To a solution of **1** (280 mg, 0.3 mmol) in DMF (3 mL), anhydrous zinc acetate (275 mg, 1.5 mmol) was added and stirred at 120 °C for 3 h. The red zinc porphyrin complex Zn(II)(5,10,15,20-tetrakis(4-bromophenyl)-porphyrin) (**1-Zn**) (268 mg, 90%) was obtained after being washed with deionized water and dried.

To a solution of **1-Zn** (150 mg, 0.15 mmol), 1,7-octadiyne (32 mg, 0.3 mmol), PdCl₂(PPh₃)₂ (42 mg, 0.06 mmol) and CuI (5.7 mg, 0.03 mmol) in DMSO (2 mL), TEA (1 mL) was added and the mixture was stirred at 100 °C for 30 min. The product was precipitated using CH₂Cl₂ and collected by centrifugation, which was further soaked with TFA to remove zinc. Red insoluble porphyrin-based porous organic polymer (**PPOP-2**) (105 mg, 85%) was obtained after being washed with deionized water and dried.



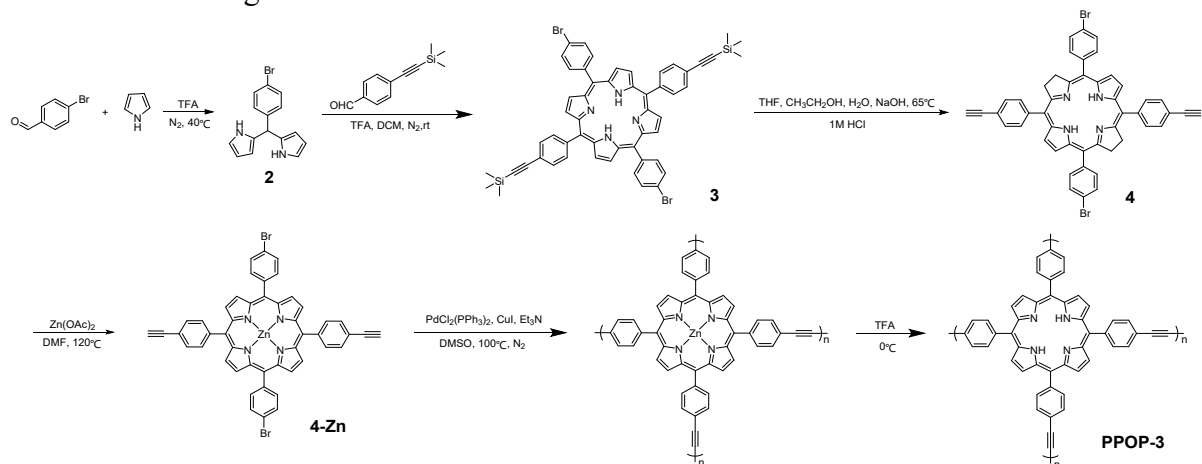
Scheme S2. Synthesis of photocatalyst PPOP-2

2.3 Synthesis of photocatalyst PPOP-3

According to reported synthetic methods,^{S2} pyrrole (5 mL, 75 mmol) and 4-bromobenzaldehyde (5 g, 30 mmol) were added to the reaction vial, followed by TFA (0.1 mL). The reaction vial was evacuated, filled with nitrogen, heated to 40 °C and the reaction was stirred for 2h. The solvent was removed to give the crude product. Via silica gel column chromatography (V_{PE}/V_{EA} = 3/1), 2,2'-[(4-bromophenyl)-methylene]-bis(1H-pyrrole) (**2**) (6.5 g, 80%) was obtained. To a solution of **2** (1 g, 5.5 mmol) and 4-(trimethylsilyl)-ethynylbenzaldehyde in DCM (160 mL), TFA (0.17 mL) was added and stirred at room

temperature under nitrogen for 3 h. Then 2,3-dichloro-5,6-dicyano-1,4-benzoquinone (DDQ) (2.7 g, 16.5 mmol) was added and stirred at room temperature for 30 min. The solvent was removed and purified via silica gel column chromatography ($V_{PE}/V_{DCM} = 2/1$) to give 4,4'-[10,20-bis(4-bromophenyl)-5,15-bis(2-ethynyltrimethylsilylphenyl)]-porphyrin (**3**) (635 mg, 24%). **3** (400 mg, 0.4 mmol) and THF (8 mL) were added to the reaction flask. After stirring to dissolve, ethanol (6 mL), deionized water (4 mL), and sodium hydroxide (80 mg, 2 mmol) were added, and stirred at 65 °C overnight. At the end of the reaction, the pH of the system was adjusted to 5-6 with 1 M hydrochloric acid solution, filtered and dried to give 4,4'-[10,20-bis(4-bromophenyl)-5,15-bis(2-ethynylphenyl)]-porphyrin (**4**) (296 mg, 90%). To a solution of **4** (200 mg, 0.24 mmol) in DMF (3 mL), anhydrous zinc acetate (220 mg, 1.2 mmol) was added and stirred at 120 °C for 3 h. The red zinc porphyrin complex Zn(II)(4,4'-[10,20-bis(4-bromophenyl)-5,15-bis(2-ethynylphenyl)]-porphyrin) (**4-Zn**) (191 mg, 90%) was obtained after being washed with deionized water and dried.

To a solution of **4-Zn** (150 mg, 0.17 mmol), 1,4-diethynylbenzene (43 mg, 0.34 mmol), $PdCl_2(PPh_3)_2$ (48 mg, 0.068 mmol) and CuI (6.5 mg, 0.034 mmol) in DMSO (2 mL), TEA (1 mL) was added and the mixture was stirred at 100 °C for 30 min. The product was precipitated using CH_2Cl_2 and collected by centrifugation, which was further soaked with TFA to remove zinc. Red insoluble porphyrin-based porous organic polymer (**PPOP-3**) (114 mg, 85%) was obtained after being washed with deionized water and dried.



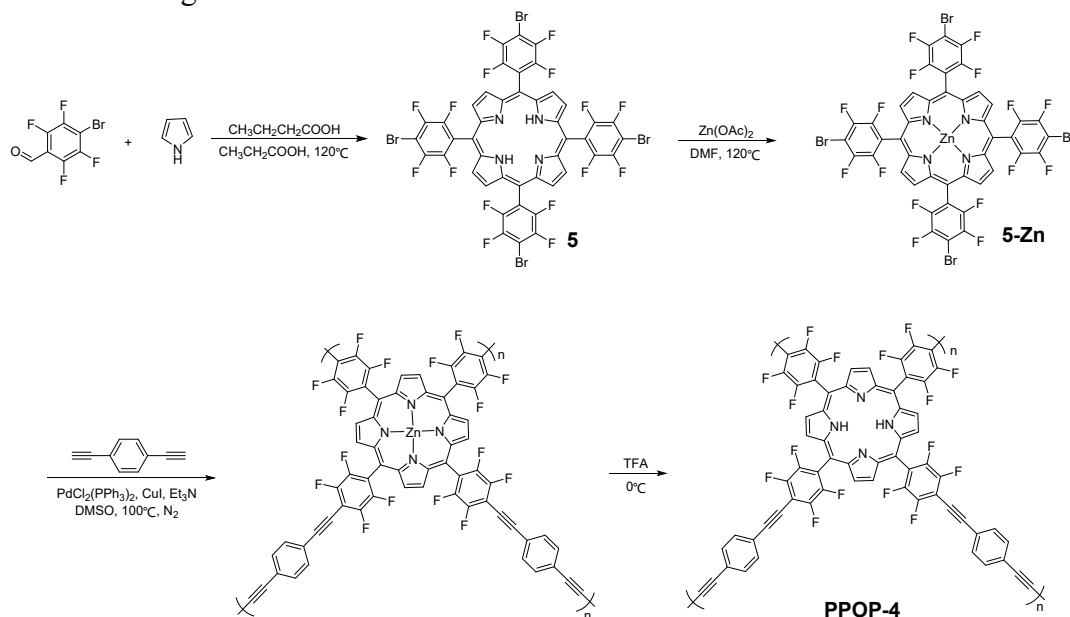
Scheme S3. Synthesis of photocatalyst **PPOP-3**

2.4 Synthesis of photocatalyst PPOP-4

Pyrrole (0.27 mL, 3.9 mmol) and 4-bromo-2,3,5,6-tetrafluorobenzaldehyde (1 g, 3.9 mmol) were dissolved in the mixture of propionic acid (15 mL) containing acetic acid (5 mL), followed by stirred at 120 °C for 2 h. After cooling to room temperature, it was washed with formic acid and dried to obtain 5,10,15,20-tetrakis(4-bromo-2,3,5,6-tetrafluorophenyl)-porphyrin (**5**) (350 mg, 30%). To a solution of **5** (200 mg, 0.16 mmol) in DMF (3 mL), anhydrous zinc acetate (150 mg, 0.8 mmol) was added and stirred at 120 °C for 3 h. The red zinc porphyrin complex Zn(II)(5,10,15,20-tetrakis(4-bromo-2,3,5,6-tetrafluorophenyl)-

porphyrin) (**5-Zn**) (190 mg, 90%) was obtained after being washed with deionized water and dried.

To a solution of **5-Zn** (150 mg, 0.12 mmol), 1,4-diethynylbenzene (30 mg, 0.24 mmol), $\text{PdCl}_2(\text{PPh}_3)_2$ (34 mg, 0.048 mmol) and CuI (4.6 mg, 0.024 mmol) in DMSO (2 mL), TEA (1 mL) was added and the mixture was stirred at 100 °C for 30 min. The product was precipitated using CH_2Cl_2 and collected by centrifugation, which was further soaked with TFA to remove zinc. Red insoluble porphyrin-based porous organic polymer (**PPOP-4**) (117 mg, 85%) was obtained after being washed with deionized water and dried.^{S3}

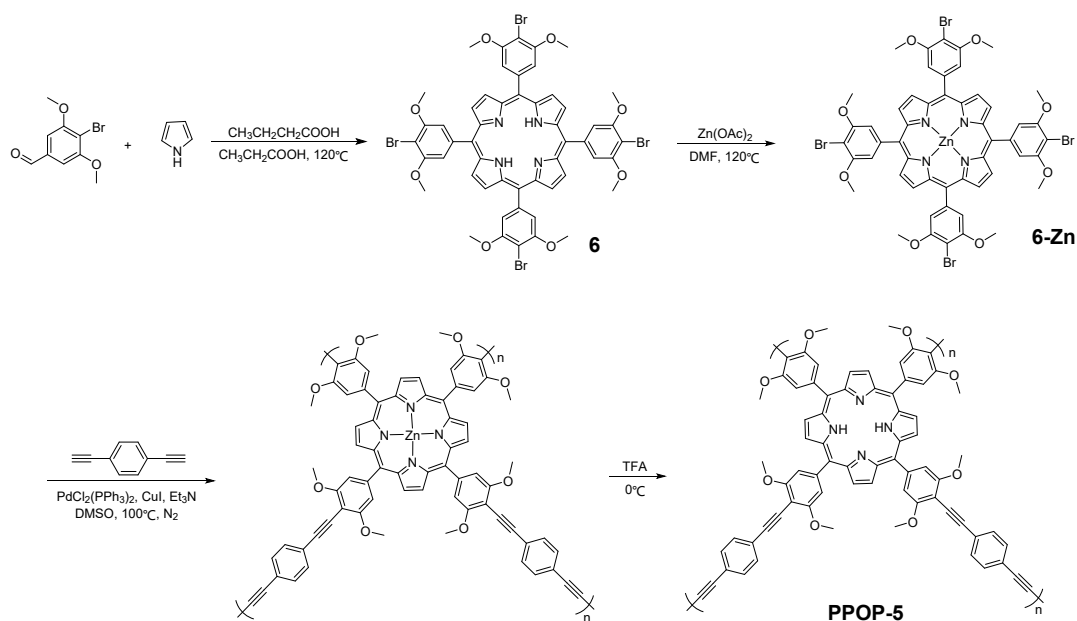


Scheme S4. Synthesis of photocatalyst **PPOP-4**

2.5 Synthesis of photocatalyst PPOP-5

Pyrrole (0.14 mL, 2 mmol) and 4-bromo-3,5-dimethoxybenzaldehyde (490 mg, 2 mmol) were dissolved in the mixture of propionic acid (15 mL) containing acetic acid (5 mL), followed by stirred at 120 °C for 2 h. After cooling to room temperature, it was washed with formic acid and dried to obtain 5,10,15,20-tetra(4-bromo-3,5-dimethoxyphenyl)-porphyrin (**6**) (293 mg, 50%). To a solution of **6** (200 mg, 0.17 mmol) in DMF (3 mL), anhydrous zinc acetate (156 mg, 0.85 mmol) was added and stirred at 120 °C for 3 h. The red zinc porphyrin complex Zn(II)(5,10,15,20-tetra(4-bromo-3,5-dimethoxyphenyl)-porphyrin) (**6-Zn**) (198 mg, 94%) was obtained after being washed with deionized water and dried.

To a solution of **6-Zn** (150 mg, 0.12 mmol), 1,4-diethynylbenzene (30 mg, 0.24 mmol), $\text{PdCl}_2(\text{PPh}_3)_2$ (34 mg, 0.048 mmol) and CuI (4.6 mg, 0.024 mmol) in DMSO (2 mL), TEA (1 mL) was added and the mixture was stirred at 100 °C for 30 min. The product was precipitated using CH_2Cl_2 and collected by centrifugation, which was further soaked with TFA to remove zinc. Red insoluble porphyrin-based porous organic polymer (**PPOP-5**) (112 mg, 85%) was obtained after being washed with deionized water and dried.



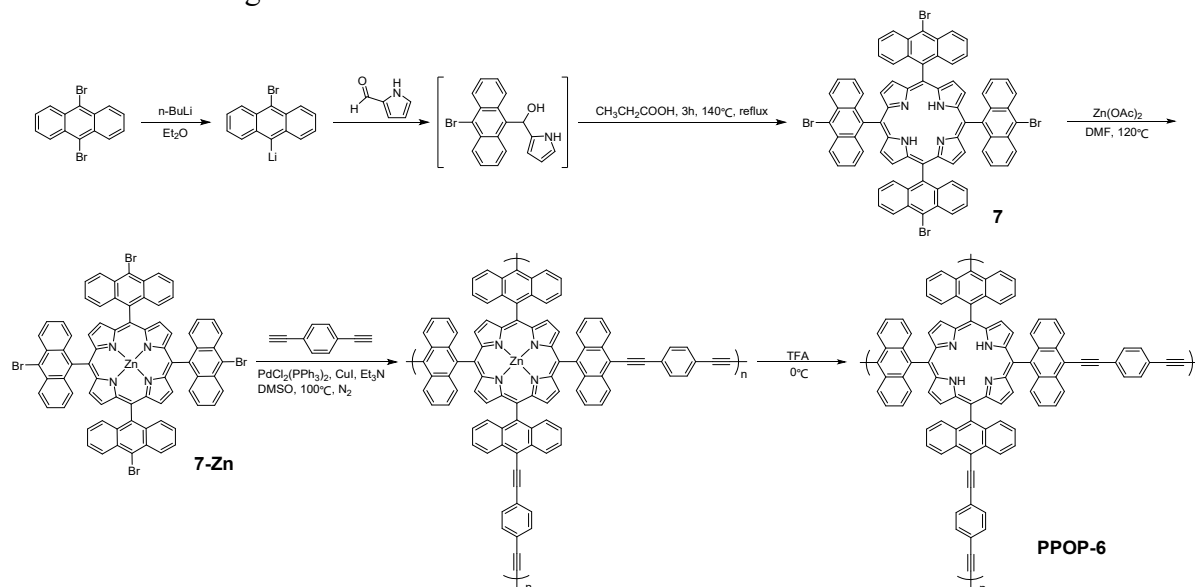
Scheme S5. Synthesis of photocatalyst PPOP-5

2.6 Synthesis of photocatalyst PPOP-6

According to reported synthetic methods,^{S4} to a solution of 9,10-dibromoanthracene (3 g, 8.9 mmol) in dried diethylether (15 mL) was added n-butyllithium (2 M in hexane, 4.5 mL, 9 mmol) and the mixture was stirred at room temperature for 30 min. Then, a solution of pyrrole-2-carboxaldehyde (428 mg, 4.5 mmol) in diethylether (3.5 mL) was added and the mixture was stirred at room temperature for 1 h. The intensely red mixture was poured into a cold and saturated solution of NH₄Cl (30 mL). The organic phase was separated, washed with water (3 × 30 mL) and dried over Na₂SO₄ before the solvent was removed over vacuum. The intermediary crude product was directly introduced into a boiling solution of propionic acid (25 mL), stirred for 3 h at 140 °C and allowed to cool overnight. At the end of the reaction, the black thick mixture afforded was filtered over paper filter and washed with MeOH until the elution of a clear solution. The collected precipitate was poured into MeOH (250 mL), sonicated for 2 min and filtered again. This process was repeated twice to remove the major part of polymeric side products. Then the latest precipitate was purified on a large silica column eluted with CH₂Cl₂ to collect the very first orange-red fraction. The solvent was removed and the final product was re-crystallized from CH₂Cl₂/MeOH to afford violet crystals 5,10,15,20-tetrakis(10-bromoanthracen-9-yl)-porphyrin (7) (215 mg, 15% with respect to pyrrole-2-carboxaldehyde). To a solution of 7 (200 mg, 0.15 mmol) in DMF (3 mL), anhydrous zinc acetate (138 mg, 0.75 mmol) was added and stirred at 120 °C for 3 h. The red zinc porphyrin complex Zn(II)(5,10,15,20-tetrakis(10-bromoanthracen-9-yl)-porphyrin) (7-Zn) (188 mg, 90%) was obtained after being washed with deionized water and dried.

To a solution of 7-Zn (170 mg, 0.12 mmol), 1,4-diethynylbenzene (30 mg, 0.24 mmol), PdCl₂(PPh₃)₂ (34 mg, 0.048 mmol) and CuI (4.6 mg, 0.024 mmol) in DMSO (2 mL), TEA (1 mL) was added and the mixture was stirred at 100 °C for 30 min. The product was precipitated using CH₂Cl₂ and collected by centrifugation, which was further soaked with TFA to remove

zinc. Red insoluble porphyrin-based porous organic polymer (**PPOP-6**) (128 mg, 85%) was obtained after being washed with deionized water and dried.

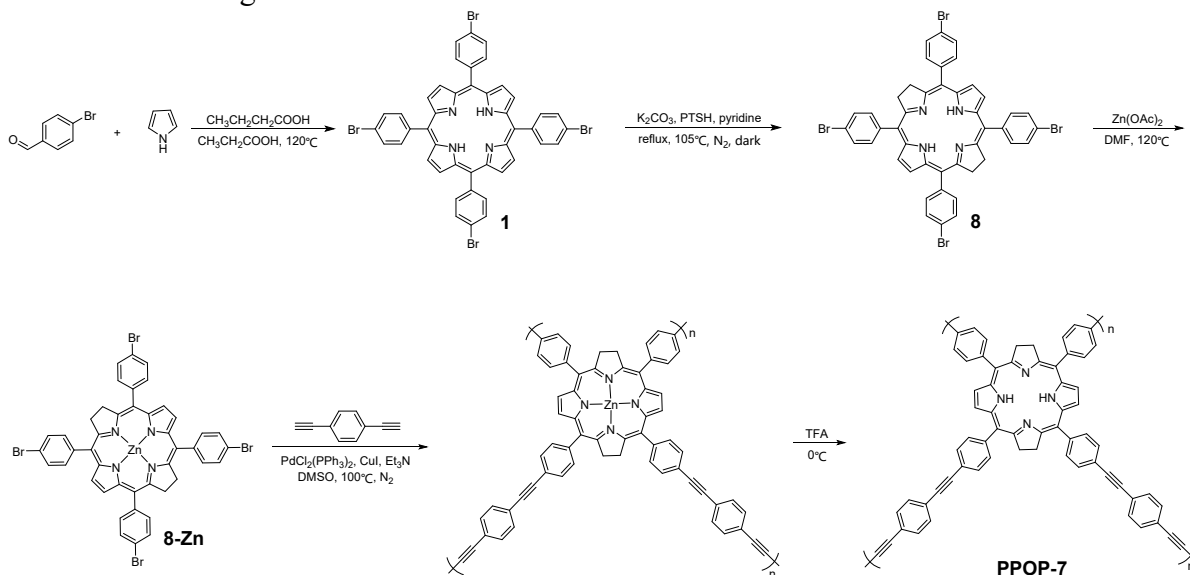


Scheme S6. Synthesis of photocatalyst **PPOP-6**

2.7 Synthesis of photocatalyst **PPOP-7**

Pyrrole (2 mL, 30 mmol) and 4-bromobenzaldehyde (5 g, 30 mmol) were dissolved in the mixture of propionic acid (45 mL) containing acetic acid (15 mL), followed by stirred at 120 °C for 2 h. After cooling to room temperature, it was washed with formic acid and dried to obtain 5,10,15,20-tetrakis(4-bromophenyl)-porphyrin (**1**) (5.65 g, 90%). According to reported synthetic methods,^{S5} **1** (400 mg, 0.43 mmol), anhydrous potassium carbonate (890 mg, 6.4 mmol) and 50 mL anhydrous pyridine were mixed in 500 mL three-necked flask under nitrogen protection. After all the solids dissolved, p-toluenesulfonyl hydrazide (PTSH) (800 mg, 4.3 mmol) was added, and the reaction mixture was kept stirring with the exclusion of light and heated under reflux at 105 °C for 20 h. After the end of the reflux, under the protection of nitrogen, the equal amount of PTSH was added to the reaction mixture, and then stirred for another 8 h at ambient temperature in the dark. Then 50 mL of benzene and 50 mL of deionized water were added to mixture under reflux for 1 h. After cooling, the organic phase was extracted once with HCl (about 2 M) and extracted with 68% phosphoric acid two times, and then extracted once with water, with saturated sodium bicarbonate solution two times. After dried with sodium sulfate, the solution was removed by a rotary evaporator. The crude product was purified via silica gel column chromatography ($V_{PE}/V_{DCM} = 2/1$) to obtain a black solid 7,8,17,18-tetrahydro-5,10,15,20-tetrakis(4-bromophenyl)-21H,23H-porphine (**8**) (200 mg, 50%). To a solution of **8** (200 mg, 0.21 mmol) in DMF (3 mL), anhydrous zinc acetate (200 mg, 1.05 mmol) was added and stirred at 120 °C for 3 h. The blue-green zinc porphyrin complex Zn(II)(7,8,17,18-tetrahydro-5,10,15,20-tetrakis(4-bromophenyl)-21H,23H-porphine) (**8-Zn**) (198 mg, 93%) was obtained after being washed with deionized water and dried.

To a solution of **8-Zn** (150 mg, 0.15 mmol), 1,4-diethynylbenzene (38 mg, 0.3 mmol), $\text{PdCl}_2(\text{PPh}_3)_2$ (42 mg, 0.06 mmol) and CuI (5.7 mg, 0.03 mmol) in DMSO (2 mL), TEA (1 mL) was added and the mixture was stirred at 100 °C for 30 min. The product was precipitated using CH_2Cl_2 and collected by centrifugation, which was further soaked with TFA to remove zinc. Red insoluble porphyrin-based porous organic polymer (**PPOP-7**) (117 mg, 85%) was obtained after being washed with deionized water and dried.



Scheme S7. Synthesis of photocatalyst **PPOP-7**

3. Analysis and characterization of photocatalyst PPOP-1

Firstly, we had systematically characterized the chemical structure and properties of **PPOP-1**. Fourier-transformed infrared spectrum (FT-IR) verified that all the typical peaks for porphyrins remained and the signal at around 2200 cm^{-1} representing the internal alkyne appeared (**Figure S1**). Scanning electron microscopy (SEM) image indicated that **PPOP-1** owned the spherical structure with the particle size around 250 nm (**Figure S2**). The pore size and Brunauer-Emmett-Teller (BET) surface areas of **PPOP-1** were characterized to be 33 nm and $7.24\text{ m}^2\text{g}^{-1}$ by measuring the N_2 adsorption-desorption at 77 K , which was typical mesoporous structure with a type III isotherm (**Figure S3**). The ultraviolet–visible absorption spectrum (UV-vis) of **PPOP-1** showed that the photocatalyst had absorption in the black light region (**Figure S4**). The X-ray diffraction (XRD) results showed the amorphous structure of **PPOP-1** (**Figure S5**). The thermal stability of **PPOP-1** was evaluated using thermogravimetric analysis (TGA) and the results displayed that **PPOP-1** could tolerate the temperature as high as $200\text{ }^\circ\text{C}$ (**Figure S5**).

3.1 Fourier-transformed infrared spectrum of photocatalyst PPOP-1

We tested the Fourier-transformed infrared spectrum of **PPOP-1**. There are absorption peaks at 1600 cm^{-1} for the benzene ring, at 1486 cm^{-1} for the backbone vibration of the porphyrin ring, at 1340 cm^{-1} for the stretching vibration of the C-N bond, and at 2200 cm^{-1} for the stretching vibration of the $\text{C}\equiv\text{C}$ bond.

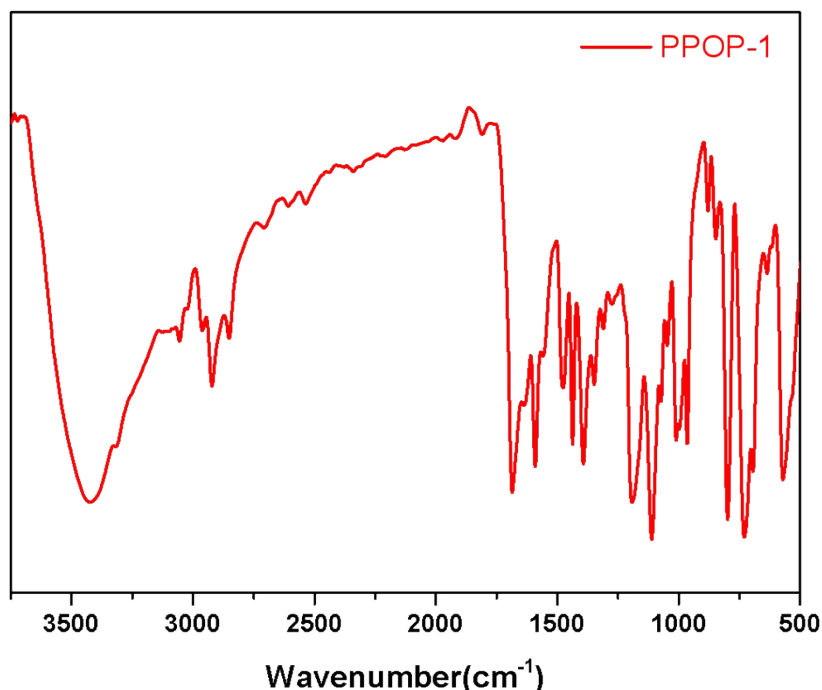


Figure S1. FT-IR spectrum of photocatalyst **PPOP-1**.

3.2 SEM image of photocatalyst PPOP-1

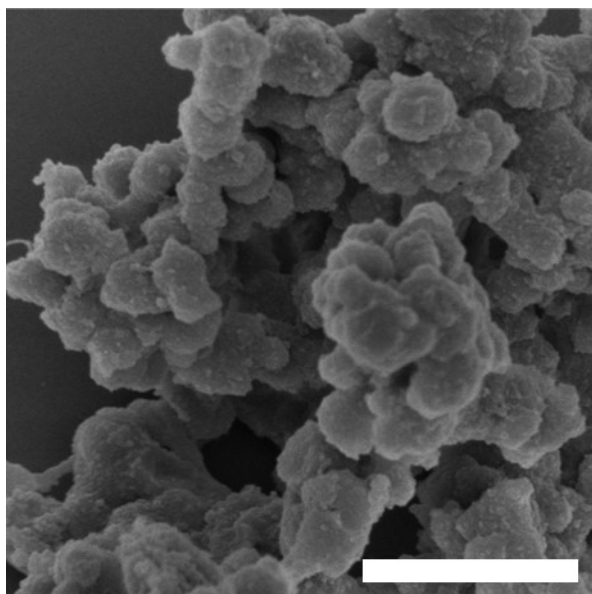


Figure S2. SEM image of PPOP-1. Bar = 1 μm .

3.3 BET surface areas of photocatalyst PPOP-1

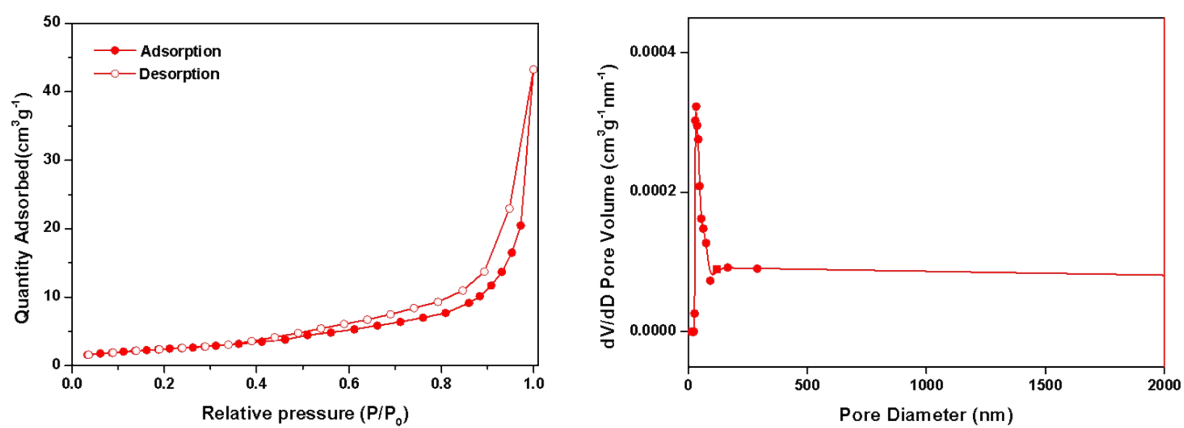


Figure S3. N_2 adsorption-desorption isotherms and pore size distributions of PPOP-1.

3.4 UV-vis spectrum of photocatalyst PPOP-1

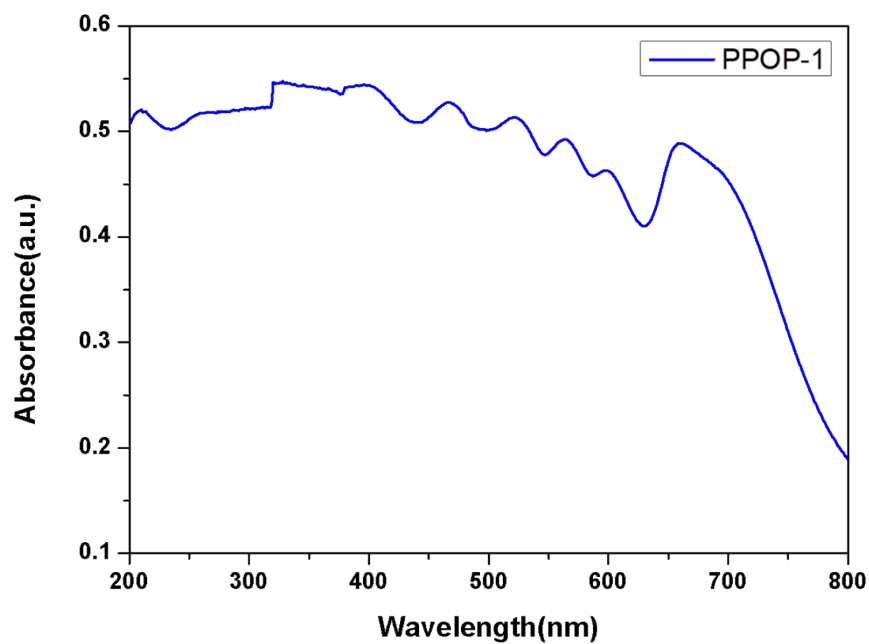


Figure S4. Solid UV-vis spectrum of PPOP-1.

3.5 X-ray diffraction patterns of photocatalyst PPOP-1

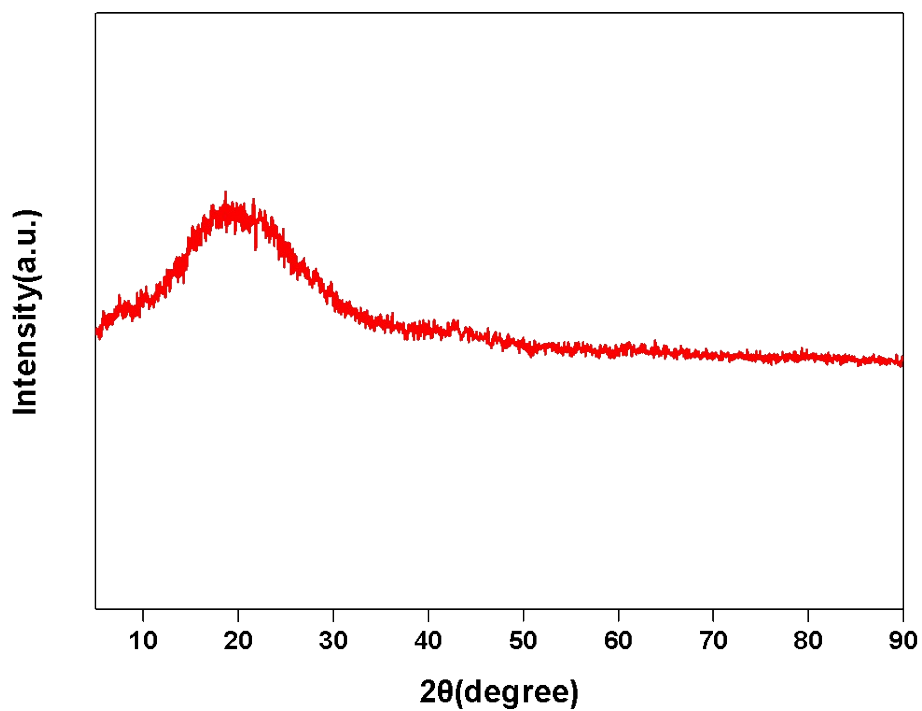


Figure S5. XRD patterns of PPOP-1.

3.6 Thermogravimetric analysis image of photocatalyst PPOP-1

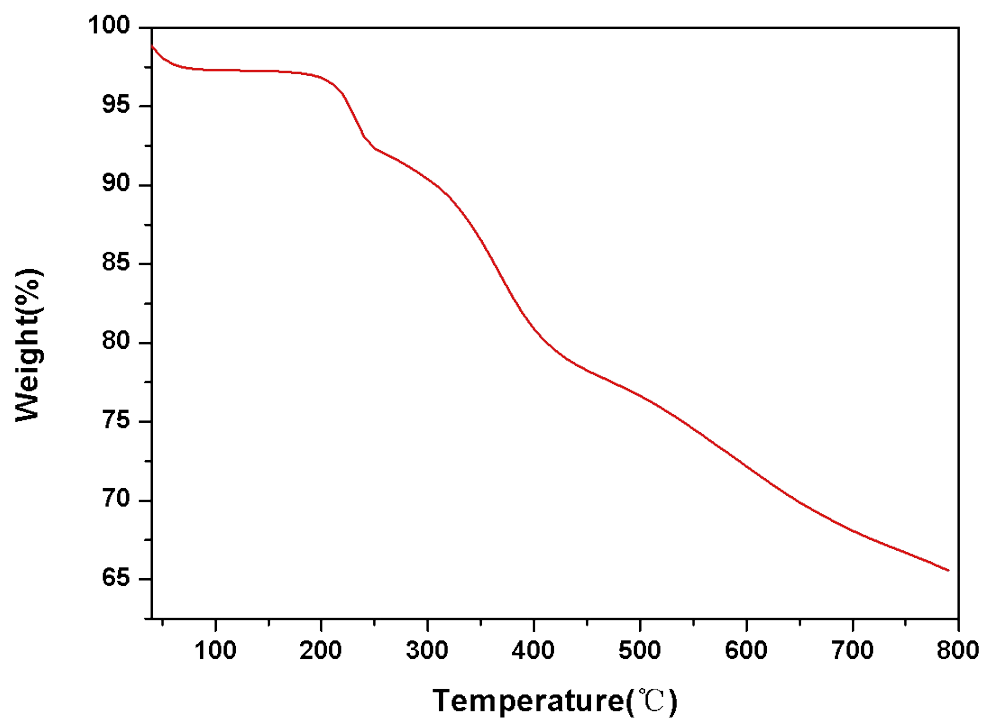


Figure S6. TGA image of PPOP-1.

4. Details of photoreactor

The photocatalytic reactions were performed on WATTCAS Parallel Light Reactor (WP-TEC-1020HSL) with 20 W 365-370 nm black COB LED.

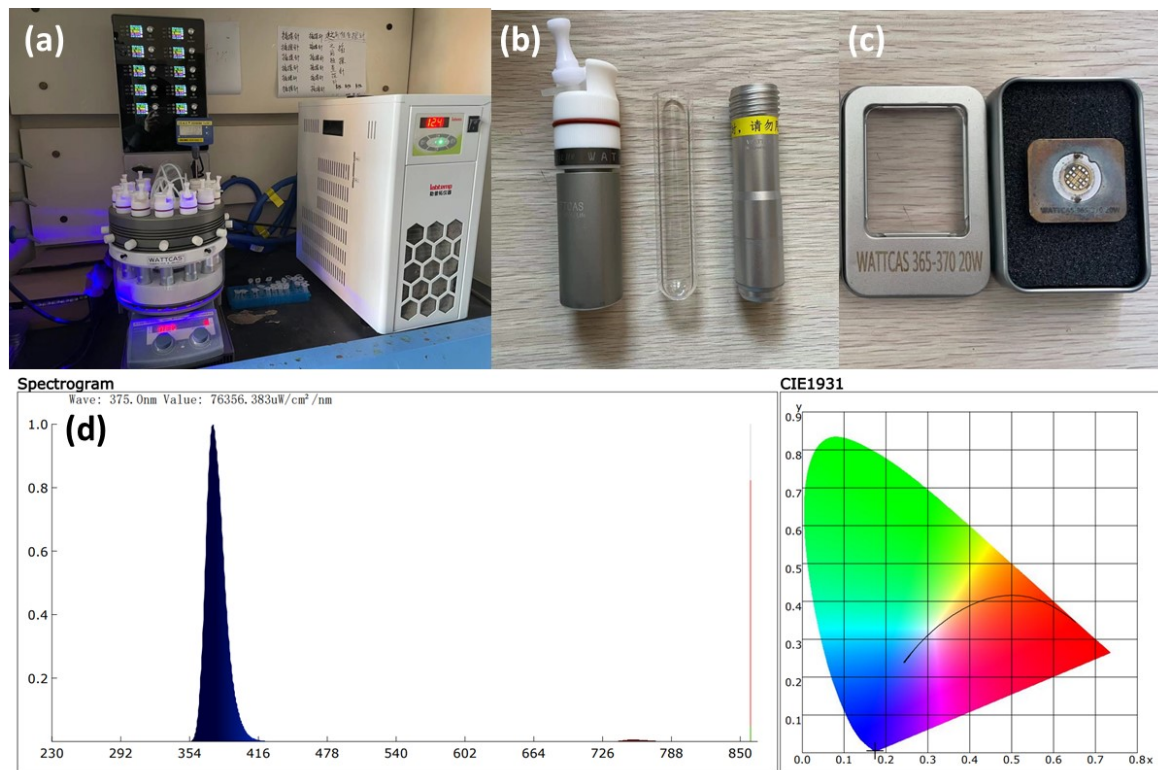
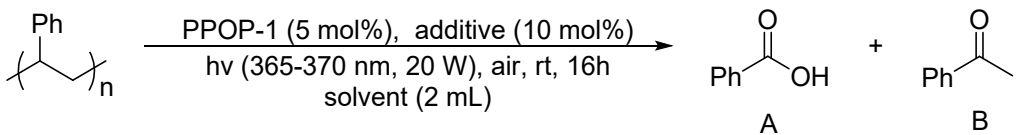


Figure S7. (a): photoreactor; (b): reaction vial; (c): chip; (d): spectrum of 365-370nm black LED light.

5. Optimization of reaction conditions

Table S1. Optimization of the Reaction Conditions^{a,b}



Entry	PPOP-1 (mol%)	Additive (mol%)	Solvent	Yield of A (%) ^c	Yield of B (%) ^c
1	PPOP-1 (5)	<i>p</i> -TsOH·H ₂ O (10)	EtOAc	49(48)	7
2 ^d	PPOP-1 (5)	<i>p</i> -TsOH·H ₂ O (10)	EtOAc	no reaction	no reaction
3 ^e	PPOP-1 (5)	<i>p</i> -TsOH·H ₂ O (10)	EtOAc	no reaction	no reaction
4 ^f	PPOP-1 (5)	<i>p</i> -TsOH·H ₂ O (10)	EtOAc	21	5
5 ^g	PPOP-1 (5)	<i>p</i> -TsOH·H ₂ O (10)	EtOAc	trace	trace
6 ^h	PPOP-1 (5)	<i>p</i> -TsOH·H ₂ O (10)	EtOAc	no reaction	no reaction
7	PPOP-1 (5)	-	EtOAc	26	3
8	-	<i>p</i> -TsOH·H ₂ O (10)	EtOAc	18	4
9	PPOP-1 (5)	<i>p</i> -TsOH·H ₂ O (10)	DCM	trace	trace
10	PPOP-1 (5)	<i>p</i> -TsOH·H ₂ O (10)	DCE	44	5
11	PPOP-1 (5)	<i>p</i> -TsOH·H ₂ O (10)	acetone	27	7
12	PPOP-1 (5)	<i>p</i> -TsOH·H ₂ O (10)	MeCN	trace	trace
13	PPOP-1 (5)	<i>p</i> -TsOH·H ₂ O (10)	DMC	45	11
14	PPOP-1 (5)	<i>p</i> -TsOH·H ₂ O (10)	benzene	no reaction	no reaction
15	PPOP-1 (5)	<i>p</i> -TsOH·H ₂ O (10)	THF	no reaction	no reaction
16	PPOP-1 (5)	<i>p</i> -TsOH·H ₂ O (10)	1,4-Dioxane	no reaction	no reaction
17	PPOP-1 (1)	<i>p</i> -TsOH·H ₂ O (10)	EtOAc	35	7
18	PPOP-1 (2.5)	<i>p</i> -TsOH·H ₂ O (10)	EtOAc	44	6
19	PPOP-1 (10)	<i>p</i> -TsOH·H ₂ O (10)	EtOAc	50	10
20	PPOP-1 (5)	<i>p</i> -TsOH·H ₂ O (2.5)	EtOAc	28	4
21	PPOP-1 (5)	<i>p</i> -TsOH·H ₂ O (5)	EtOAc	38	7
22	PPOP-1 (5)	<i>p</i> -TsOH·H ₂ O (20)	EtOAc	50	12
23	PPOP-1 (5)	<i>p</i> -TsOH·H ₂ O (50)	EtOAc	51	12
24	PPOP-1 (5)	H ₂ SO ₄ (10)	EtOAc	35	6

25	PPOP-1 (5)	HCl (10)	EtOAc	35	3
26	PPOP-1 (5)	H ₃ PO ₄ (10)	EtOAc	22	4
27	PPOP-1 (5)	CF ₃ COOH (10)	EtOAc	26	5
28	PPOP-1 (5)	CF ₃ SO ₃ H (10)	EtOAc	29	3
29	PPOP-1 (5)	FeCl ₃ (10)	EtOAc	12	4
30	PPOP-1 (5)	ZnCl ₂ (10)	EtOAc	37	3
31	PPOP-1 (5)	Yb(OTf) ₃ (10)	EtOAc	33	5
32	PPOP-1 (5)	Sc(OTf) ₃ (10)	EtOAc	36	5
33	PPOP-1 (5)	CuOTf (10)	EtOAc	26	6
34 ⁱ	PPOP-1 (5)	<i>p</i> -TsOH·H ₂ O (10)	EtOAc	55	8
35^j	PPOP-1 (5)	<i>p</i>-TsOH·H₂O (10)	EtOAc	63(62)	3

^aReaction was carried out with polystyrene (0.2 mmol based on C₈H₈ as the repeating unit of polystyrene, 1.0 equiv) in the presence of 5 mol% PPOP-1 and 10 mol% additive in 2 mL solvent under air, black light (365-370 nm, 20 W) and room temperature for 16 h. ^bThe amounts of PPOP-1, additive and the yield of products are based on the repeating unit of polystyrene. ^cYield was determined by crude ¹H NMR spectrum with 1,3,5-trimethoxybenzene as an internal standard; isolated yield in parentheses. ^dNo light for 16 h. ^eN₂ instead of air for 16 h. ^fBlack light (365-370 nm, 10 W) was used. ^gBlue light (425-430 nm, 20 W) was used. ^hWhite light (6000-6500 K, 20 W) was used. ⁱRoom temperature for 32 h. ^jRoom temperature for 48 h.

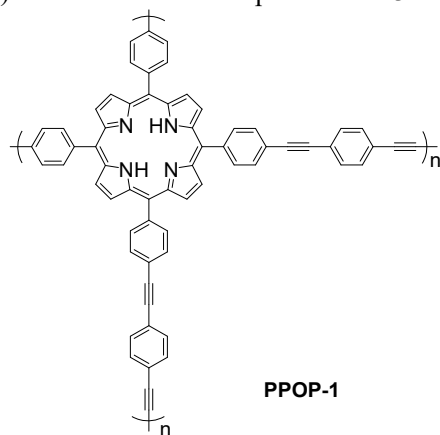


Figure S8. Structure of **PPOP-1**.

Different kinds of commercial available small-molecule photosensitizers were used, including tetrabutylammonium decatungstate (TBADT),^{S6} 9-mesityl-10-methylacridinium tetrafluoroborate (Mes-Acr-MeBF₄),^{S7} 1,2,3,5-tetrakis(carbazol-9-yl)-4,6-dicyanobenzene (4CzIPN),^{S8} tris(2,2'-bipyridyl)ruthenium(II) dichloride hexahydrate (Ru(bpy)₃(Cl)₂·6H₂O),^{S9} and bis[2-(2,4-difluorophenyl)-5-trifluoromethylpyridine][2-2'-bipyridyl]iridium hexafluorophosphate ([Ir(dF(CF₃)ppy)₂(dtbbpy)]PF₆).^{S10}

Table S2. Optimization of Various Photocatalysts^a

Entry	Photocatalyst	Yield of A (%) _b	Yield of B (%) ^b
1	TBADT	25	6
2	Mes-Acr-MeBF ₄	36	5
3	4CzIPN	13	6
4	Ru(bpy) ₃ (Cl) ₂ ·6H ₂ O	trace	trace
5	(Ir[dF(CF ₃)ppy] ₂ (dtbbpy))PF ₆	trace	trace
6	TPP	17	5
7	T CPP	15	3
8	PPOP-1	63(62)	3
9	PPOP-2	61	3
10	PPOP-3	60	1
11	PPOP-4	62	1
12	PPOP-5	61	2
13	PPOP-6	65	5
14	PPOP-7	71(71)	2

^aReaction conditions: polystyrene (0.2 mmol based on C₈H₈ as the repeating unit of polystyrene, 1.0 equiv), photocatalyst (0.01 mmol, 5 mol%), p-TsOH·H₂O (0.02 mmol, 10mol %), EtOAc (2.0 mL), black light (365-370 nm, 20 W), open in air, and room temperature for 48 h. ^bYield was determined by crude ¹H NMR spectrum with 1,3,5-trimethoxybenzene as an internal standard; isolated yield in parentheses.

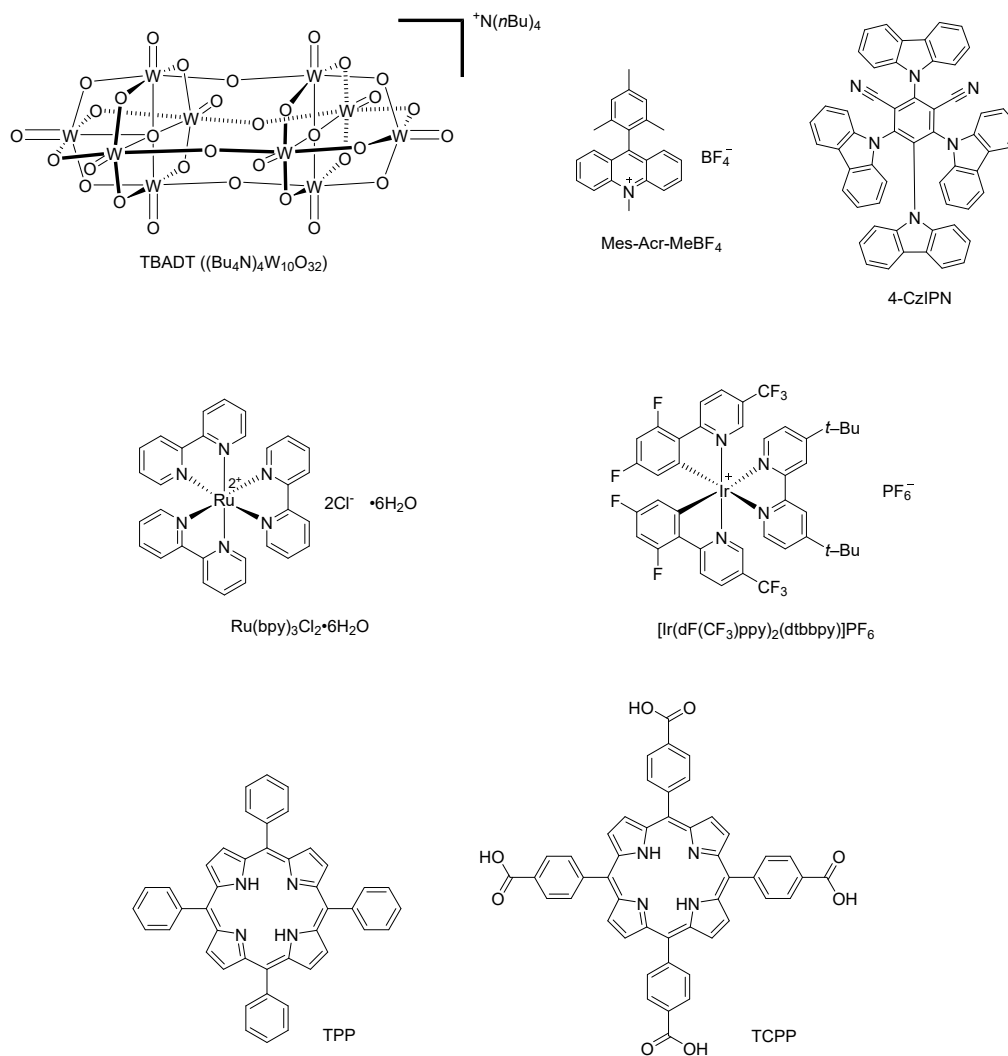


Figure S9. Structures of small-molecule photocatalysts.

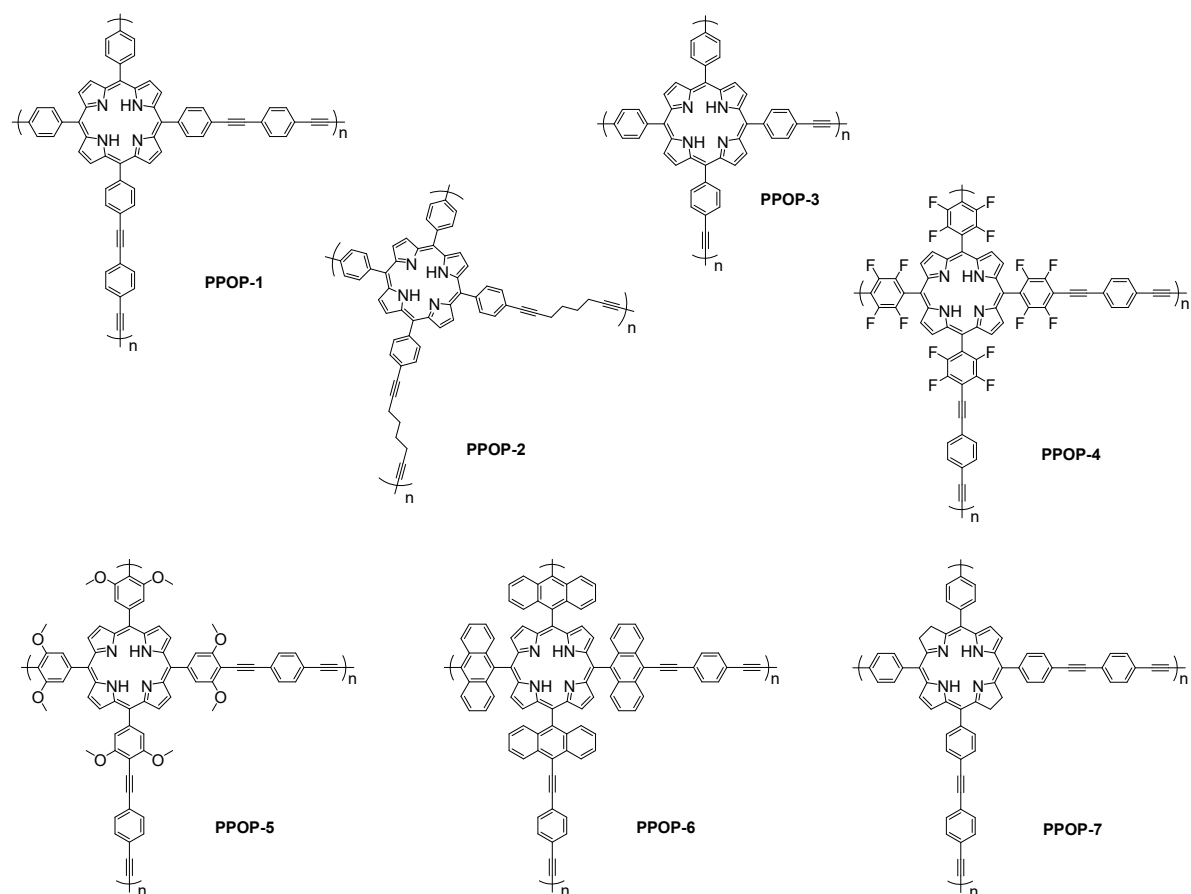


Figure S10. Structures of photocatalysts PPOPs.

6. Analysis and characterization of photocatalyst PPOP-7

We had systematically characterized the chemical structure and properties of **PPOP-7**. 7,8,17,18-tetrahydro-5,10,15,20-tetrakis(4-bromophenyl)-21H,23H-porphine (**8**), one of the polymerized monomers of **PPOP-7**, is obtained by reduction of 5,10,15,20-tetrakis(4-bromophenyl)-porphyrin (**1**). The ultraviolet–visible absorption spectra (UV/vis) of **1** and **8** showed that **8** had stronger absorption than **1** in the black light region (**Figure S11**). Fourier-transformed infrared spectrum (FT-IR) verified that all the typical peaks for porphyrins remained and the signal at around 2200 cm^{-1} representing the internal alkyne appeared (**Figure S12**). Scanning electron microscopy (SEM) image indicated that **PPOP-7** owned the spherical structure with the particle size around 250 nm (**Figure S13**). The pore size and Brunauer-Emmett-Teller (BET) surface areas of **PPOP-7** were characterized to be 2.6 nm and 270.07 m^2g^{-1} by measuring the N_2 adsorption-desorption at 77 K, which was typical mesoporous structure with a type III isotherm (**Figure S14**). The ultraviolet–visible absorption spectrum (UV-vis) of **PPOP-7** showed that the photocatalyst had absorption in the black light region (**Figure S15**). The X-ray diffraction (XRD) results showed the amorphous structure of **PPOP-7** (**Figure S16**). The thermal stability of **PPOP-7** was evaluated using thermogravimetric analysis (TGA) and the results displayed that **PPOP-7** could tolerate the temperature as high as 200 $^\circ\text{C}$ (**Figure S17**).

6.1 UV–vis spectra of **1** and **8**

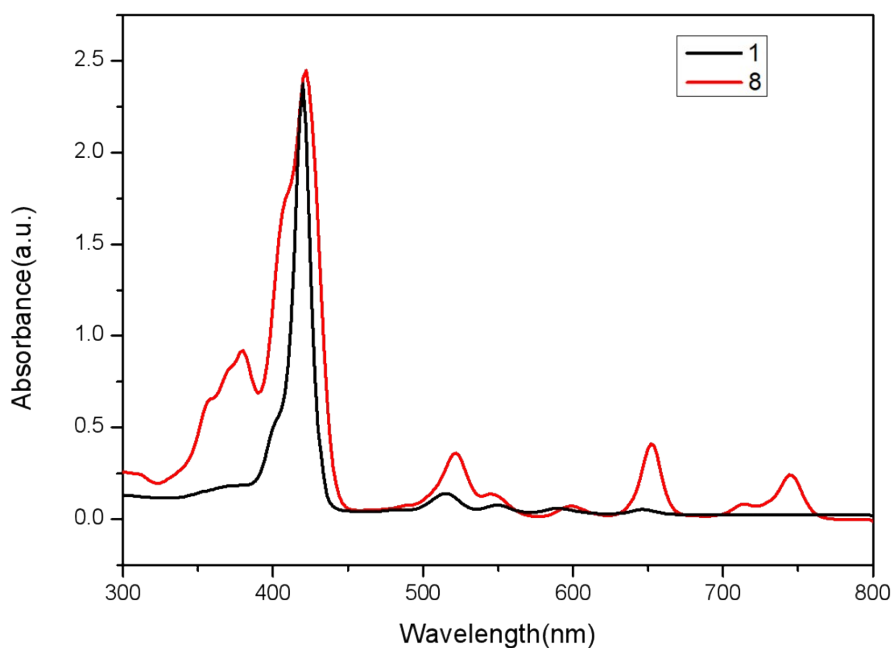


Figure S11. UV–vis spectra of **1** and **8** in DMSO.

6.2 Fourier-transformed infrared spectrum of photocatalyst PPOP-7

We tested the Fourier-transformed infrared spectrum of **PPOP-7**. There are absorption peaks at 1600 cm^{-1} for the benzene ring, at 1486 cm^{-1} for the backbone vibration of the porphyrin ring, at 1340 cm^{-1} for the stretching vibration of the C-N bond, and at 2200 cm^{-1} for the stretching vibration of the $\text{C}\equiv\text{C}$ bond.

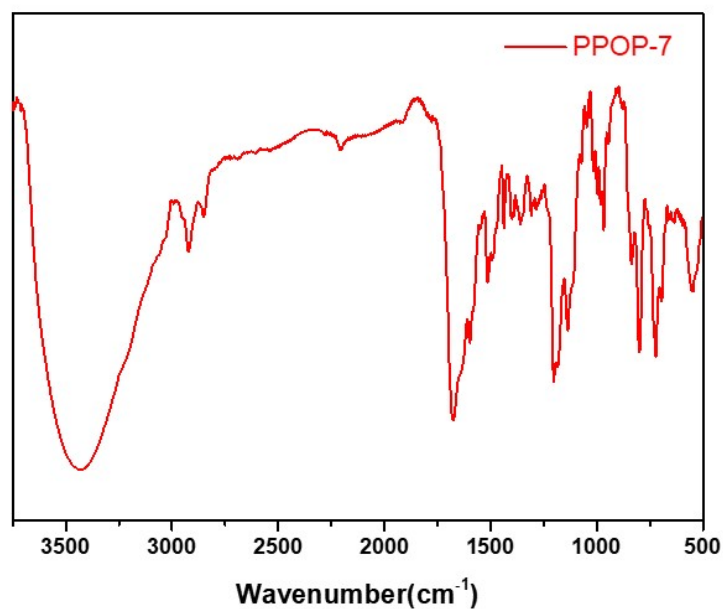


Figure S12. FT-IR spectrum of photocatalyst **PPOP-7**.

6.3 SEM image of photocatalyst PPOP-7

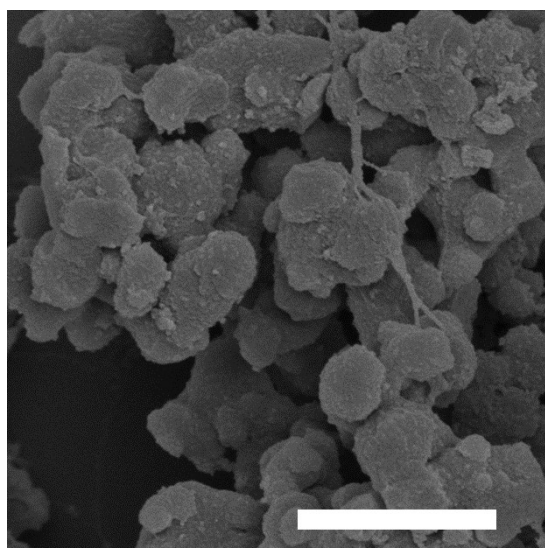


Figure S13. SEM image of **PPOP-7**. Bar = $1\text{ }\mu\text{m}$.

6.4 BET surface areas of photocatalyst PPOP-7

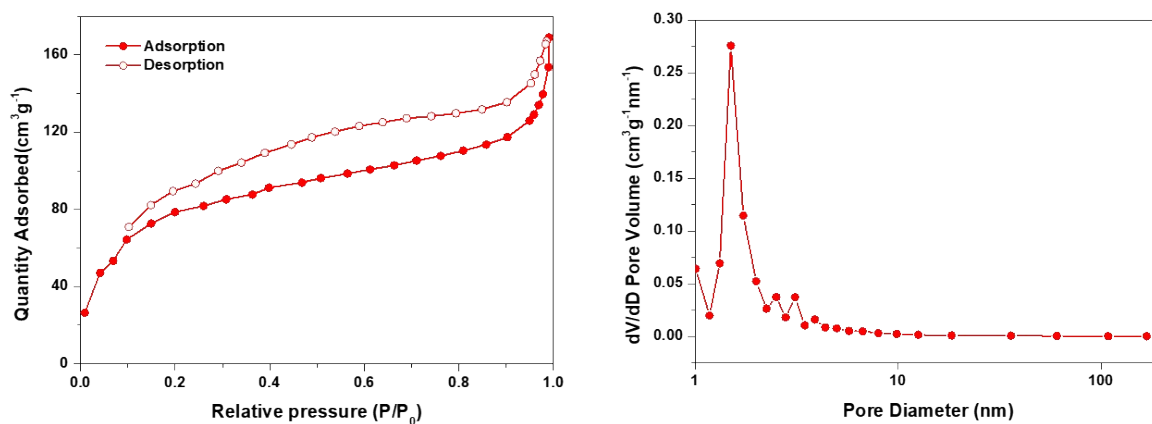


Figure S14. N₂ adsorption-desorption isotherms and pore size distributions of PPOP-7.

6.5 UV-vis spectrum of photocatalyst PPOP-7

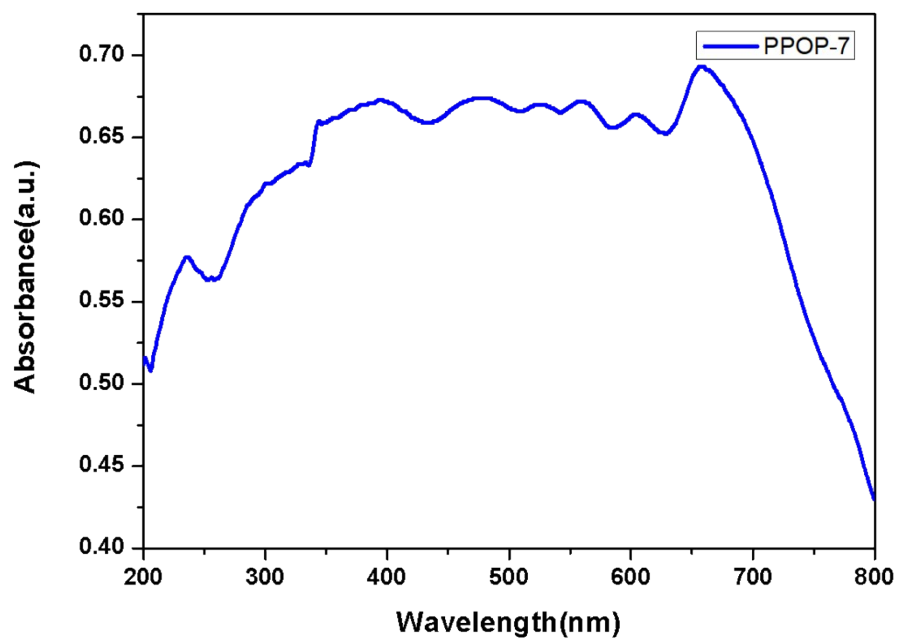


Figure S15. Solid UV-vis spectrum of PPOP-7.

6.6 X-ray diffraction patterns of photocatalyst PPOP-7

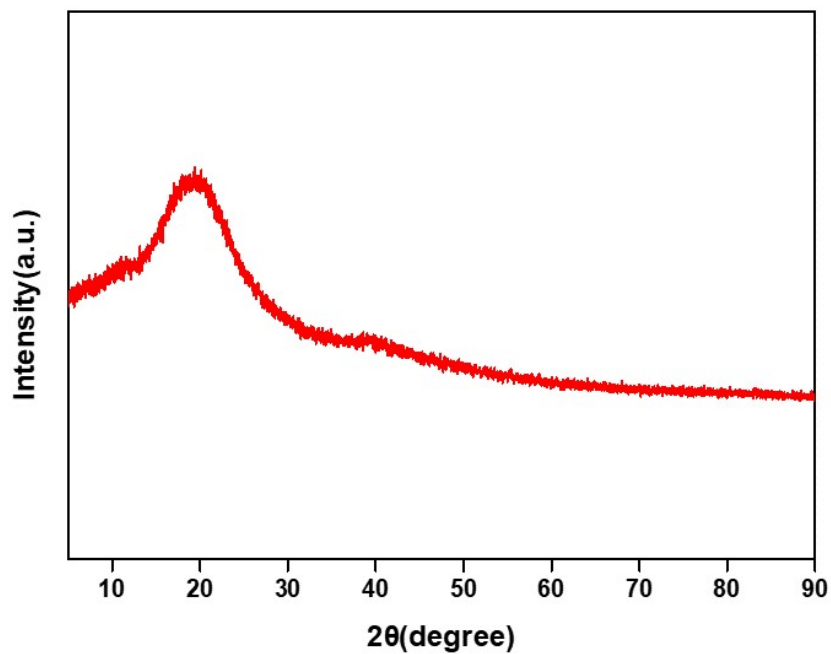


Figure S16. XRD patterns of PPOP-7.

6.7 Thermogravimetric analysis image of photocatalyst PPOP-7

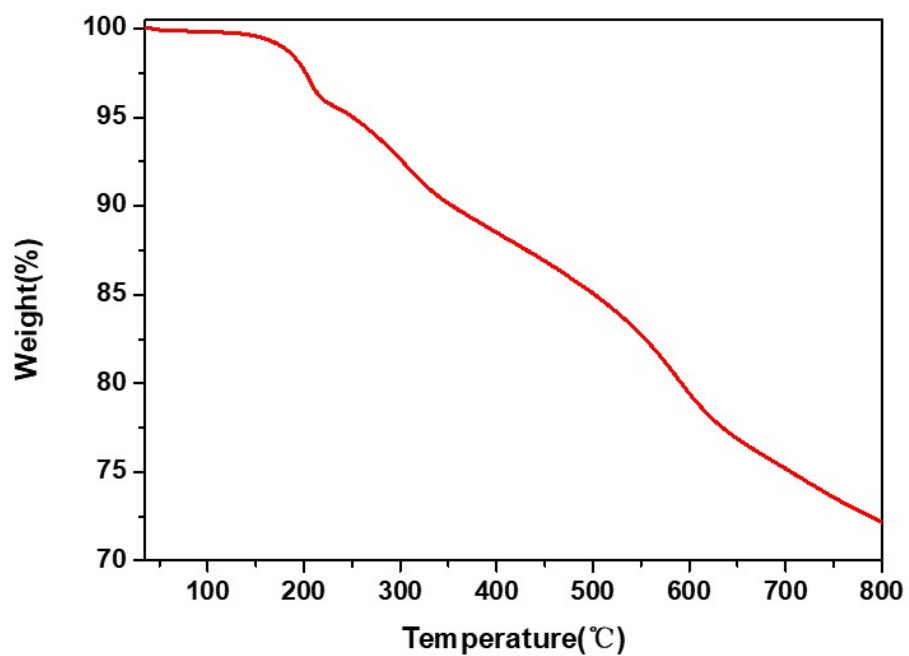
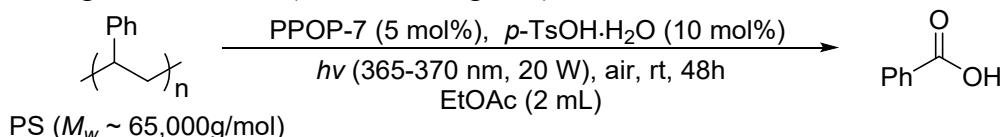


Figure S17. TGA image of PPOP-7.

7. Aerobic degradation of different types of polymers

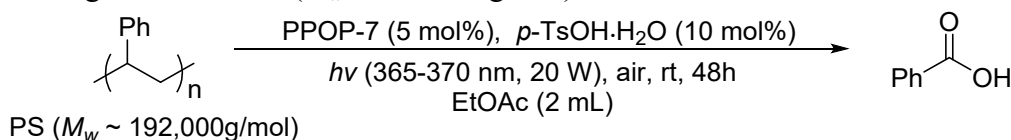
7.1 Aerobic degradation of PS

1) Aerobic degradation of PS ($M_w \sim 65,000$ g/mol)



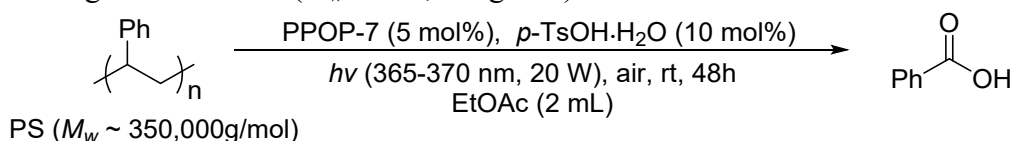
In the parallel reactor, a mixture of PS ($M_w \sim 65,000$ g/mol) (20.8 mg, 0.2 mmol based on C_8H_8 as the repeating unit of PS), PPOP-7 (8.6 mg, 5 mol%), and p -TsOH· H_2O (3.8 mg, 10 mol%) in EtOAc (2.0 mL) was stirred under air at room temperature for 48 h while being exposed to black light (365-370 nm, 20 W). The reaction was detected by TLC (PE/EA = 1:1), and the solvent was removed to afford the crude product. Benzoic acid (17.6 mg, 72% yield) was obtained through silica gel column chromatography ($V_{PE}/V_{EA} = 10/1$ to 5/1) as a white solid.

2) Aerobic degradation of PS ($M_w \sim 192,000$ g/mol)



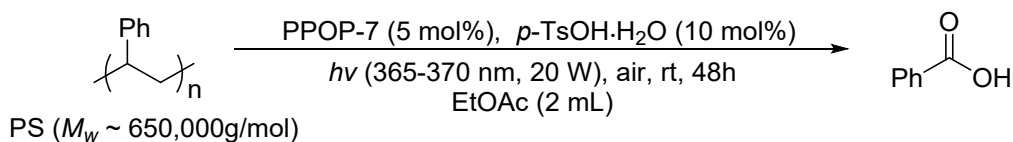
In the parallel reactor, a mixture of PS ($M_w \sim 192,000$ g/mol) (20.8 mg, 0.2 mmol based on C_8H_8 as the repeating unit of PS), PPOP-7 (8.6 mg, 5 mol%), and p -TsOH· H_2O (3.8 mg, 10 mol%) in EtOAc (2.0 mL) was stirred under air at room temperature for 48 h while being exposed to black light (365-370 nm, 20 W). The reaction was detected by TLC (PE/EA = 1:1), and the solvent was removed to afford the crude product. Benzoic acid (17.4 mg, 71% yield) was obtained through silica gel column chromatography ($V_{PE}/V_{EA} = 10/1$ to 5/1) as a white solid.

3) Aerobic degradation of PS ($M_w \sim 350,000$ g/mol)



In the parallel reactor, a mixture of PS ($M_w \sim 350,000$ g/mol) (20.8 mg, 0.2 mmol based on C_8H_8 as the repeating unit of PS), PPOP-7 (8.6 mg, 5 mol%), and p -TsOH· H_2O (3.8 mg, 10 mol%) in EtOAc (2.0 mL) was stirred under air at room temperature for 48 h while being exposed to black light (365-370 nm, 20 W). The reaction was detected by TLC (PE/EA = 1:1), and the solvent was removed to afford the crude product. Benzoic acid (17.3 mg, 71% yield) was obtained through silica gel column chromatography ($V_{PE}/V_{EA} = 10/1$ to 5/1) as a white solid.

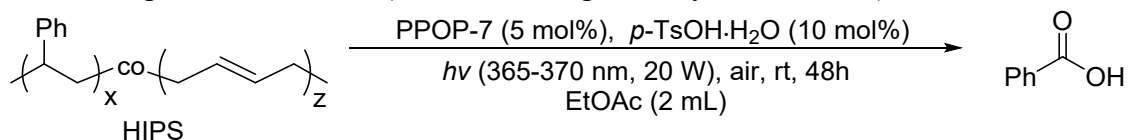
4) Aerobic degradation of PS ($M_w \sim 650,000$ g/mol)



In the parallel reactor, a mixture of PS ($M_w \sim 650,000$ g/mol) (20.8 mg, 0.2 mmol based on C_8H_8 as the repeating unit of PS), PPOP-7 (8.6 mg, 5 mol%), and p -TsOH· H_2O (3.8 mg, 10 mol%) in EtOAc (2.0 mL) was stirred under air at room temperature for 48 h while being exposed to black light (365-370 nm, 20 W). The reaction was detected by TLC (PE/EA = 1:1), and the solvent was removed to afford the crude product. Benzoic acid (16.9 mg, 69% yield) was obtained through silica gel column chromatography ($V_{PE}/V_{EA} = 10/1$ to 5/1) as a white solid.

7.2 Aerobic degradation of HIPS

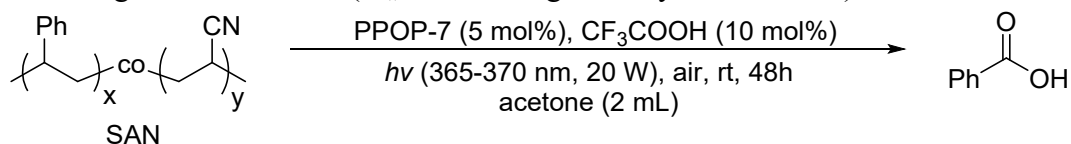
1) Aerobic degradation of HIPS ($M_w \sim 140,000$ g/mol, styrene 30 wt.%)



In the parallel reactor, a mixture of HIPS ($M_w \sim 140,000$ g/mol, styrene 30 wt.%) (69.3 mg, 0.2 mmol based on C_8H_8 as the repeating unit of PS), PPOP-7 (8.6 mg, 5 mol%), and p -TsOH· H_2O (3.8 mg, 10 mol%) in EtOAc (2.0 mL) was stirred under air at room temperature for 48 h while being exposed to black light (365-370 nm, 20 W). The reaction was detected by TLC (PE/EA = 1:1), and the solvent was removed to afford the crude product. Benzoic acid (12.2 mg, 50% yield) was obtained through silica gel column chromatography ($V_{PE}/V_{EA} = 10/1$ to 5/1) as a white solid.

7.3 Aerobic degradation of SAN

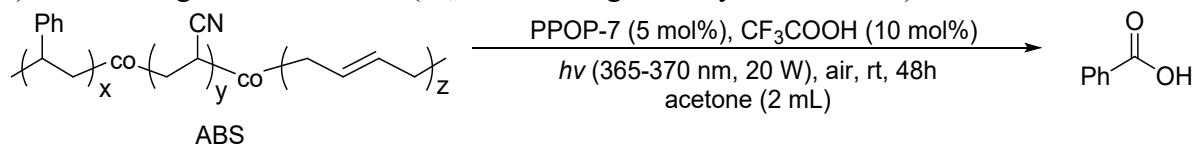
1) Aerobic degradation of SAN ($M_w \sim 165,000$ g/mol, styrene 75 wt.%)



In the parallel reactor, a mixture of SAN ($M_w \sim 165,000$ g/mol, styrene 75 wt.%) (27.7 mg, 0.2 mmol based on C_8H_8 as the repeating unit of PS), PPOP-7 (8.6 mg, 5 mol%), and CF_3COOH (2.3 mg, 10 mol%) in acetone (2.0 mL) was stirred under air at room temperature for 48 h while being exposed to black light (365-370 nm, 20 W). The reaction was detected by TLC (PE/EA = 1:1), and the solvent was removed to afford the crude product. Benzoic acid (10.3 mg, 42% yield) was obtained through silica gel column chromatography ($V_{PE}/V_{EA} = 10/1$ to 5/1) as a white solid.

7.4 Aerobic degradation of ABS

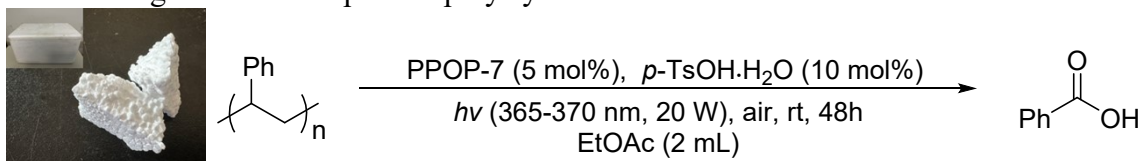
1) Aerobic degradation of ABS ($M_w \sim 238,000$ g/mol, styrene 72 wt.%)



In the parallel reactor, a mixture of ABS ($M_w \sim 238,000$ g/mol, styrene 72 wt.%) (28.9 mg, 0.2 mmol based on C_8H_8 as the repeating unit of PS), PPOP-7 (8.6 mg, 5 mol%), and CF_3COOH (2.3 mg, 10 mol%) in acetone (2.0 mL) was stirred under air at room temperature for 48 h while being exposed to black light (365-370 nm, 20 W). The reaction was detected by TLC (PE/EA = 1:1), and the solvent was removed to afford the crude product. Benzoic acid (9.8 mg, 40% yield) was obtained through silica gel column chromatography ($V_{PE}/V_{EA} = 10/1$ to 5/1) as a white solid.

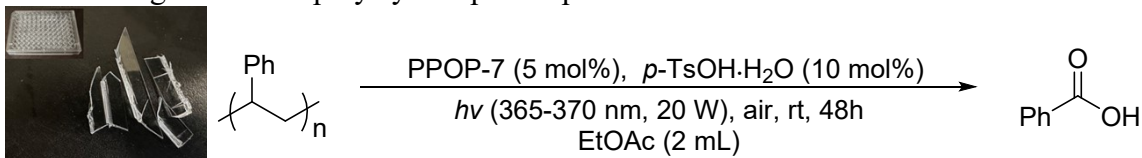
7.5 Aerobic degradation of polymer waste from our daily life

1) Aerobic degradation of expended polystyrene foam waste



In the parallel reactor, a mixture of PS waste (expended polystyrene foam waste) (20.8 mg, 0.2 mmol based on C_8H_8 as the repeating unit of PS), PPOP-7 (8.6 mg, 5 mol%), and $p-TsOH \cdot H_2O$ (3.8 mg, 10 mol%) in EtOAc (2.0 mL) was stirred under air at room temperature for 48 h while being exposed to black light (365-370 nm, 20 W). The reaction was detected by TLC (PE/EA = 1:1), and the solvent was removed to afford the crude product. Benzoic acid (15.4 mg, 63% yield) was obtained through silica gel column chromatography ($V_{PE}/V_{EA} = 10/1$ to 5/1) as a white solid.

2) Aerobic degradation of polystyrene plastic plate waste



In the parallel reactor, a mixture of PS waste (polystyrene plastic plate waste) (20.8 mg, 0.2 mmol based on C_8H_8 as the repeating unit of PS), PPOP-7 (8.6 mg, 5 mol%), and $p-TsOH \cdot H_2O$ (3.8 mg, 10 mol%) in EtOAc (2.0 mL) was stirred under air at room temperature for 48 h while being exposed to black light (365-370 nm, 20 W). The reaction was detected by TLC (PE/EA = 1:1), and the solvent was removed to afford the

8. Characterization of PS degradation

8.1 Water contact angle measurement

PS: Polystyrene (20.8 mg, 0.2 mmol based on C_8H_8 as the repeating unit of PS), PPOP-7 (8.6 mg, 5 mol%), and *p*-TsOH·H₂O (3.8 mg, 10 mol%) in EtOAc (2.0 mL) were stirred for a certain time under air at room temperature. **PS-SC:** Polystyrene (20.8 mg, 0.2 mmol based on C_8H_8 as the repeating unit of PS), PPOP-7 (8.6 mg, 5 mol%), and *p*-TsOH·H₂O (3.8 mg, 10 mol%) in EtOAc (2.0 mL) were stirred for a certain time under air at room temperature under black light (365-370 nm, 20 W) in a parallel reactor. After reacting for a period of time, the solvent was removed and washed with water, and dried them. Water contact angle test was performed with the JCD2000D2W instrument at room temperature.

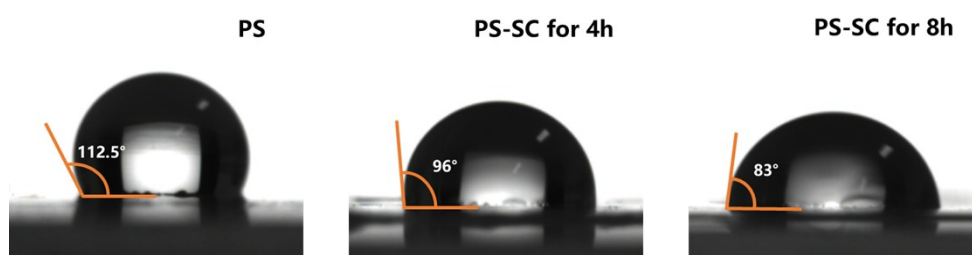


Figure S18. Comparison of water contact angles on the top surface of PS-based membranes.

8.2 X-Ray Diffraction

Polystyrene (20.8 mg, 0.2 mmol based on C_8H_8 as the repeating unit of PS), PPOP-7 (8.6 mg, 5 mol%), and *p*-TsOH·H₂O (3.8 mg, 10 mol%) in EtOAc (2.0 mL) were stirred for a certain time under air at room temperature under black light (365-370 nm, 20 W) in a parallel reactor. After a certain period, the solvent was removed and the residue was washed with water and then dried. X-Ray Diffraction of the samples obtained above was performed with the device (Ultima IV type Cu-K α).

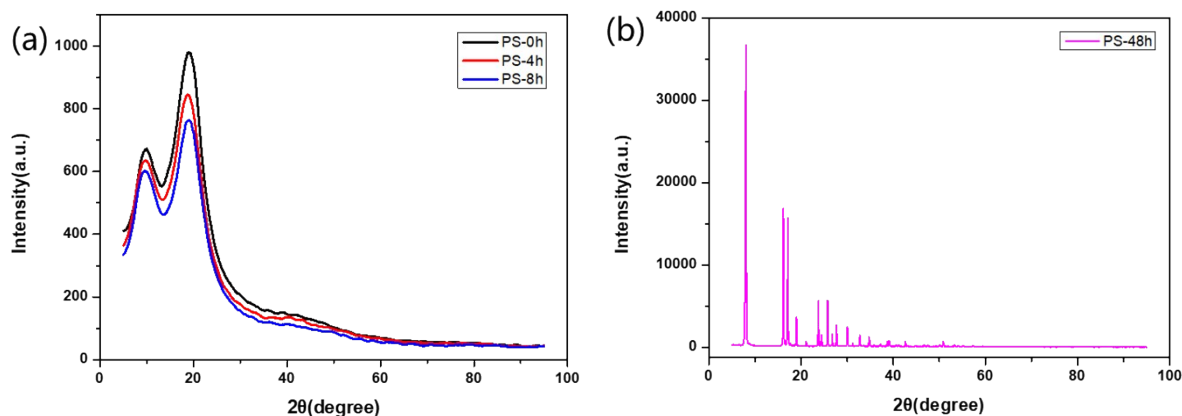


Figure S19. (a) XRD patterns of PS at different times during PS degradation; (b) XRD patterns of reaction products after 48 h of reaction

8.3 Glass transition temperature

PS-no light: Polystyrene (20.8 mg, 0.2 mmol based on C_8H_8 as the repeating unit of PS), PPOP-7 (8.6 mg, 5 mol%), and *p*-TsOH·H₂O (3.8 mg, 10 mol%) in EtOAc (2.0 mL) were stirred for a certain time under air at room temperature. **PS-SC:** Polystyrene (20.8 mg, 0.2 mmol based on C_8H_8 as the repeating unit of PS), PPOP-7 (8.6 mg, 5 mol%), and *p*-TsOH·H₂O (3.8 mg, 10 mol%) in EtOAc (2.0 mL) were stirred for a certain time under air at room temperature under black light (365-370 nm, 20 W) in a parallel reactor. After reacting for a period of time, the solvent was removed and washed with water, and dried them.

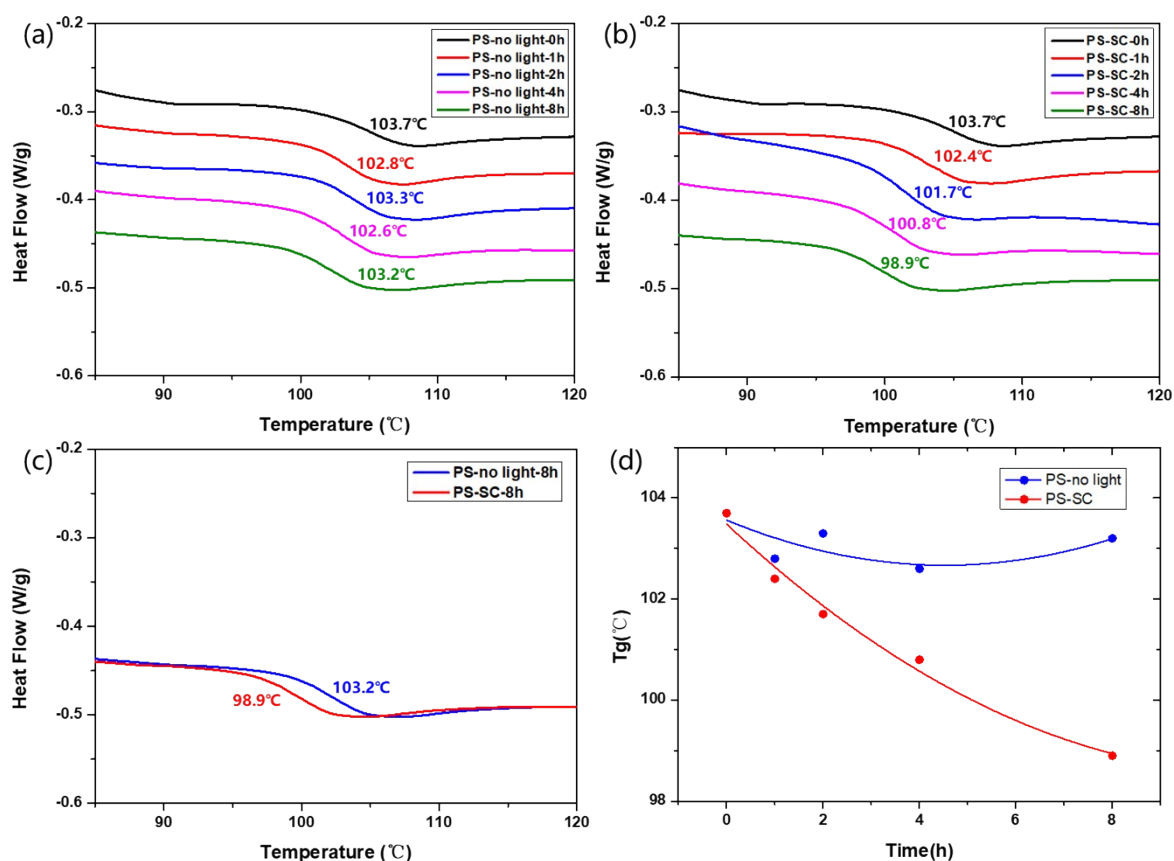


Figure S20. (a) Differential scanning calorimetry (DSC) curves at different times during PS degradation without light with their corresponding glass transition temperatures; (b) DSC curves at different times during PS degradation with standard conditions with their corresponding glass transition temperatures; (c) Differences in DSC curves and glass transition temperatures for PS degradation when reacting with or without light for 8 h; (d) Tracing of glass transition temperature for PS degradation when reacting with or without light.

8.4 GPC experiments

Prior to GPC testing, we performed a standard curve analysis using PS standard samples.

The samples (3 mg) were dissolved in *N,N*-Dimethylformamide (DMF) (2 mL) directly and filtered for GPC experiments without further operation. The procedures of sample preparation and pre-treatment were as follows.

Polystyrene (20.8 mg, 0.2 mmol based on C_8H_8 as the repeating unit of PS), PPOP-7 (8.6 mg, 5 mol%), and *p*-TsOH·H₂O (3.8 mg, 10 mol%) in EtOAc (2.0 mL) were stirred for a certain time under air at room temperature under black light (365-370 nm, 20 W) in a parallel reactor. After the reaction was completed, the solvent was removed and the residue was washed with water, then dried.

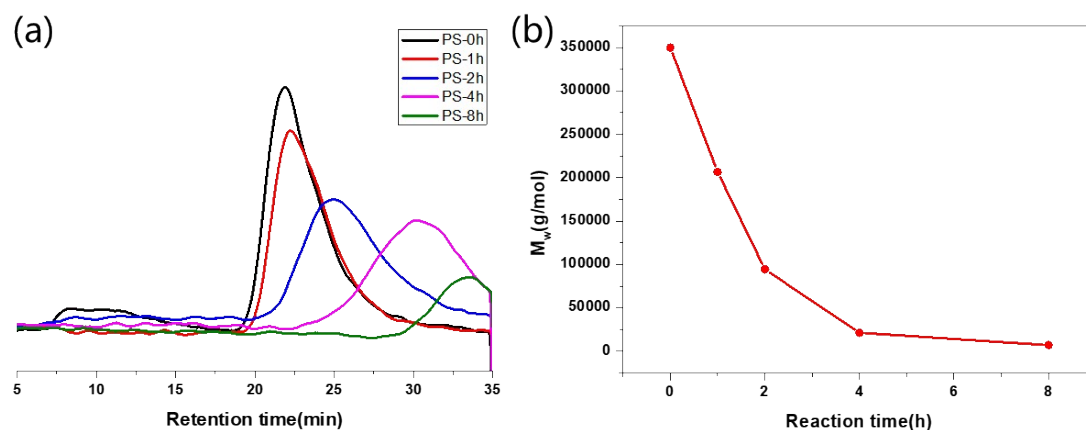


Figure S21. (a) GPC tracing experiments for PS; (b) degradation trend for PS.

9. ICP-MS determined possible metal residues of photocatalysts PPOP-1 and PPOP-7

The possible metal residues of **PPOP-1** and **PPOP-7** were almost removed from the photocatalyst, which were demonstrated by inductively coupled plasma-mass spectrometry (ICP-MS) (Table S3 and S4).

9.1 ICP-MS determined possible metal residues of photocatalyst PPOP-1

Table S3. ICP-MS determined possible metal residues of **PPOP-1**

Entry	Metal	Concentration (ppm)
1	copper ion	13.2
2	palladium ion	22.7
3	zinc ion	8.1

9.2 ICP-MS determined possible metal residues of photocatalyst PPOP-7

Table S4. ICP-MS determined possible metal residues of **PPOP-7**

Entry	Metal	Concentration (ppm)
1	copper ion	15.8
2	palladium ion	23.3
3	zinc ion	2.5

10. Comparison of reactive oxygen species yield of TPP, PPOP-1 and PPOP-7

To assess the ability of **TPP**, **PPOP-1** and **PPOP-7** to generate reactive oxygen species (ROS), 2',7'-dichlorodihydrofluorescein (DCFH) was used as a probe.^{S11} **TPP**, **PPOP-1** and **PPOP-7** were dispersed separately into water and sonicated into a homogeneous suspension (1 μM based on the porphyrin unit). A solution of this probe in water (10 μM) was added to the above suspension. The mixtures were then exposed to light (365-370 nm, 20 W) irradiation for different periods of time, at which the fluorescence intensity (at 500-700 nm) was measured using the multifunctional enzyme marker Synergy H1 (BioTek, USA). The intensity at 525 nm was used to quantify the rate of generation of ROS.

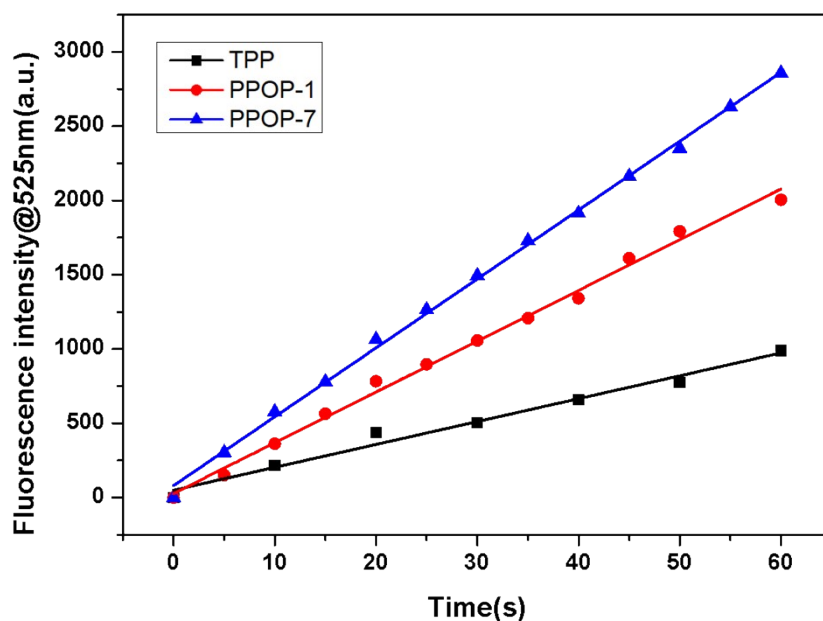


Figure S22. Comparison of the rate of increase in fluorescence intensity of 2',7'-dichlorofluorescein (DCF) at 525 nm of **TPP**, **PPOP-1** and **PPOP-7** in water (both at 1 μM) upon light (365-370 nm, 20 W) irradiation. The initial concentration of DCFH was fixed at 10 μM .

11. UV–vis spectra of photocatalysts PPOP-2, PPOP-3, PPOP-4, PPOP-5 and PPOP-6

The ultraviolet–visible absorption spectra (UV-vis) of other five PPOPs, including **PPOP-1**, **PPOP-3**, **PPOP-4**, **PPOP-5** and **PPOP-6**, showed that the photocatalysts both had absorption in the black light region. Some reports on the relevant characterization of the PPOPs are also available.^{S1-S4,S12}

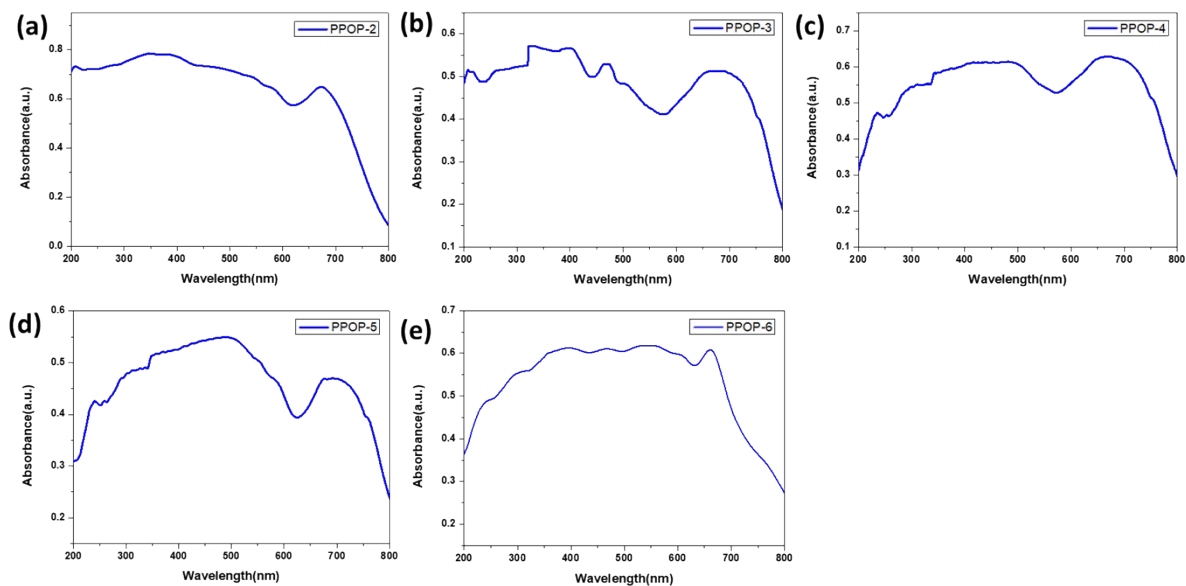


Figure S23. Solid UV–vis spectra of (a)**PPOP-2**, (b)**PPOP-3**, (c)**PPOP-4**, (d)**PPOP-5** and (e)**PPOP-6**.

12. UV-vis spectra of photocatalyst PPOP-7 at different times of reaction

In the parallel reactor, a mixture of PS (20.8 mg, 0.2 mmol based on C_8H_8 as the repeating unit of PS), PPOP-7 (8.6 mg, 5 mol%), and *p*-TsOH·H₂O (3.8 mg, 10 mol%) in EtOAc (2.0 mL) was stirred under air at room temperature while being exposed to black light (365-370 nm, 20 W). After reacting for a period of time, **PPOP-7** was obtained by centrifugation, washed with EtOAc and then dried. Then we tested the UV-vis absorption of **PPOP-7**. The UV-vis absorption images of **PPOP-7** at different reaction times were compared together. From the UV-vis absorption spectra, it could be seen that **PPOP-7** had no obvious changes or photo-corrosion during the reaction process, which proved that **PPOP-7** had a good stability.

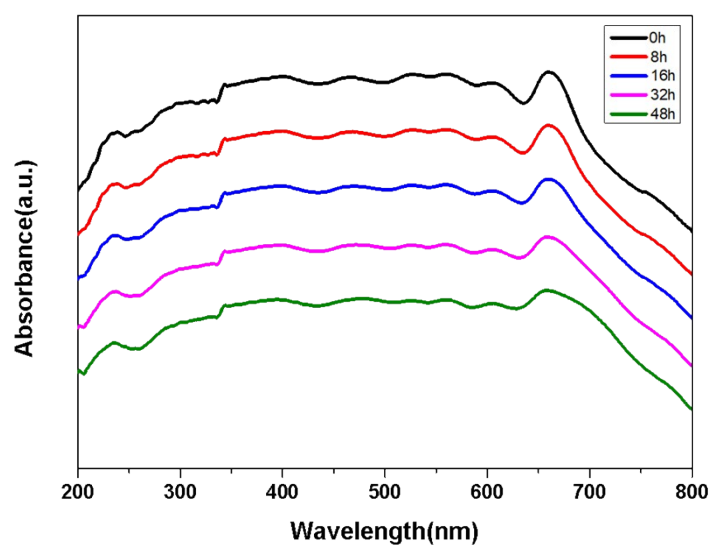
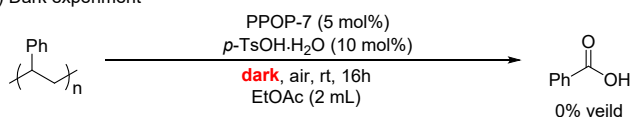


Figure S24. Solid UV-vis spectra of **PPOP-7** at different times of reaction.

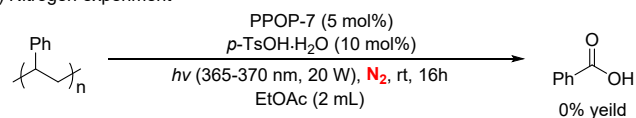
13. Control experiments

Some control experiments were systemically carried out to probe the photocatalytic mechanism. The reaction failed to occur without light or air (**Scheme S8a-S8b**). When all other conditions were kept constant but no additive was used, benzoic acid could still be produced but at a reduced rate (**Scheme S8c**). Similarly, when all other conditions were kept constant but no photocatalyst was used, benzoic acid could still be produced but at a reduced rate (**Scheme S8d**). When NaN_3 (50 mol%) was used as a singlet oxygen scavenger, almost no desired product can be observed (**Scheme S8e**). When 9,10-diphenylanthracene (DPA) (50 mol%) was used as a singlet oxygen trap, almost no desired product can be observed (**Scheme S8f**). When TEMPO (50 mol%) was used as a radical scavenger, almost no desired product can be observed (**Scheme S8g**). It indicated that singlet oxygen might have been involved in the reaction and triggered the form of free radicals that facilitated PS degradation to produce benzoic acid.

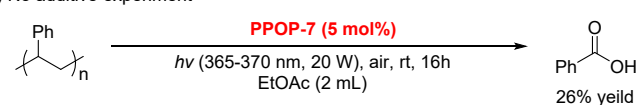
(a) Dark experiment



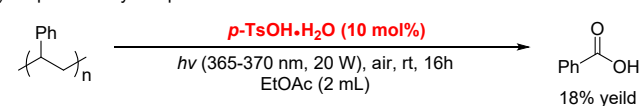
(b) Nitrogen experiment



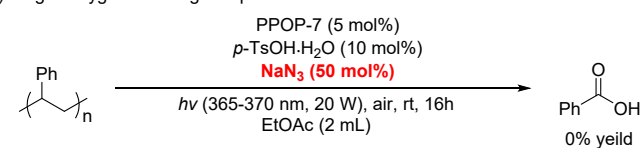
(c) No additive experiment



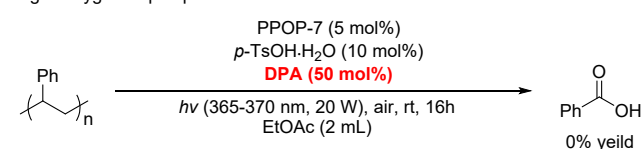
(d) No photocatalyst experiment



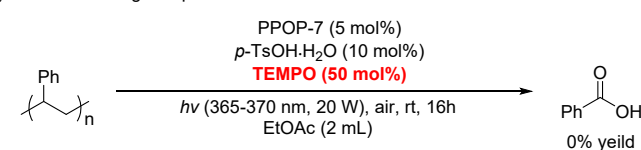
(e) Singlet oxygen scavenger experiment



(f) Singlet oxygen trap experiment



(g) Radical scavenger experiment



Scheme S8. Control experiment for the degradation of PS

We proposed the mechanism basing on the presence of benzoyl formic acid according to the reference.^{S13} To verify the presence of benzoyl formic acid, a validation experiment was performed. In the parallel reactor, a mixture of PS (20.8 mg, 0.2 mmol based on C₈H₈ as the repeating unit of PS), PPOP-7 (8.6 mg, 5 mol%), and *p*-TsOH·H₂O (3.8 mg, 10 mol%) in EtOAc (2.0 mL) was stirred under air at room temperature while being exposed to black light (365-370 nm, 20 W). After stirring the reaction for 8 h, the reaction solution was filtered and dried. The reacted mixture was measured by HRMS and benzoyl formic acid could be found.

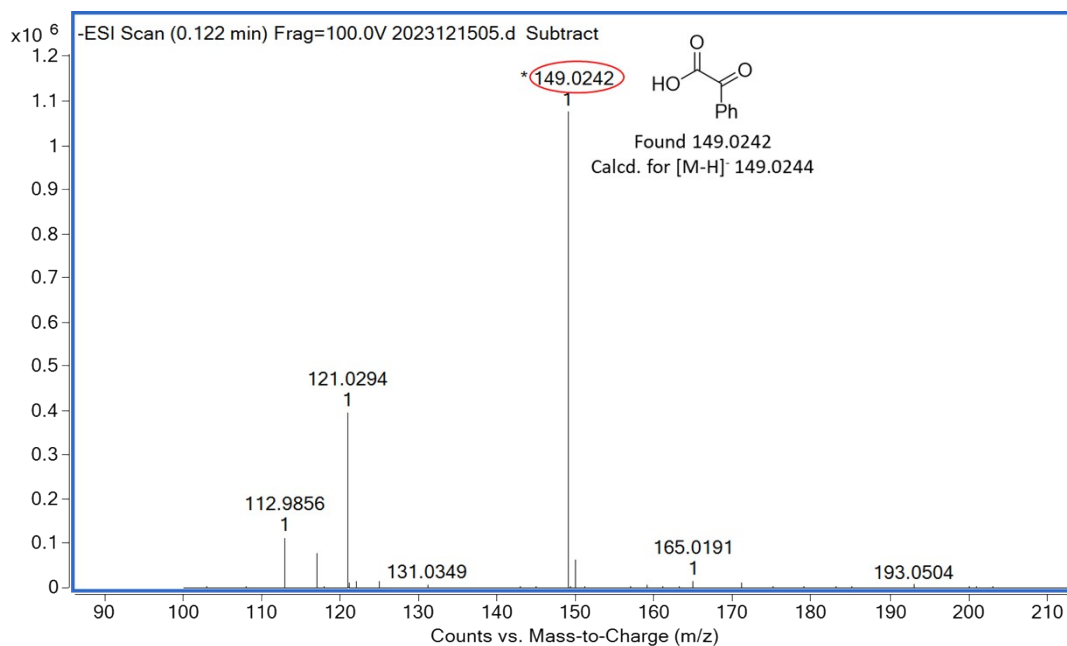
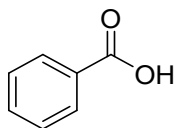


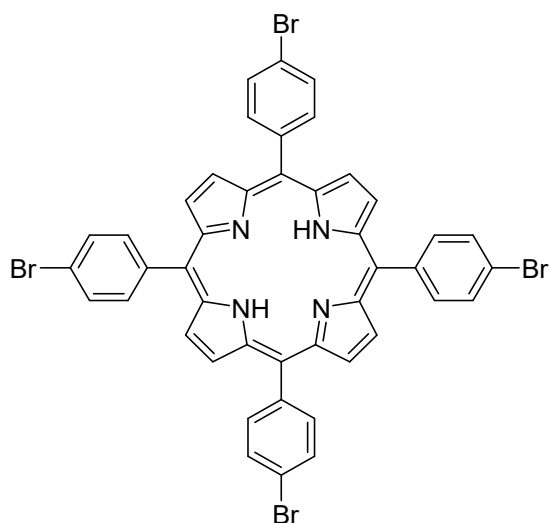
Figure S25. HRMS of benzoyl formic acid.

HRMS (ESI-TOF, *m/z*): [M-H]⁻ calcd for C₈H₆O₃, 149.0244; found, 149.0242.

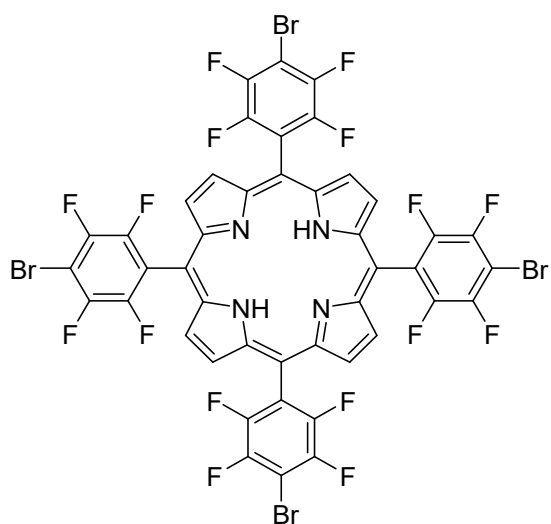
14. Characterization data



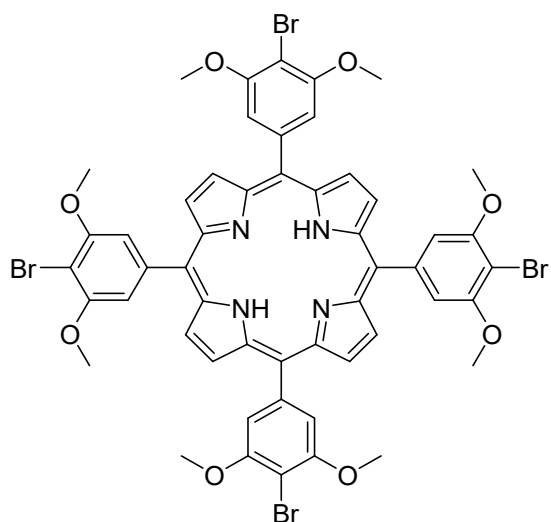
Benzoic acid.^{S14} White solid; ¹H NMR (400 MHz, CDCl₃) δ 11.72 (s, 1H), 8.14 (d, *J* = 7.9 Hz, 2H), 7.63 (t, *J* = 7.4 Hz, 1H), 7.49 (t, *J* = 7.7 Hz, 2H).



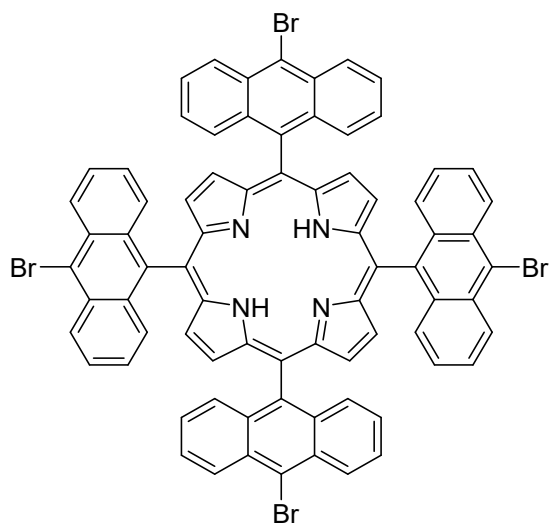
5,10,15,20-tetrakis(4-bromophenyl)-porphyrin (**1**).^{S12} Purple solid; ¹H NMR (400 MHz, CDCl₃) δ 8.84 (s, 8H), 8.07 (d, *J* = 8.2 Hz, 8H), 7.90 (d, *J* = 8.2 Hz, 8H), -2.87 (s, 2H).



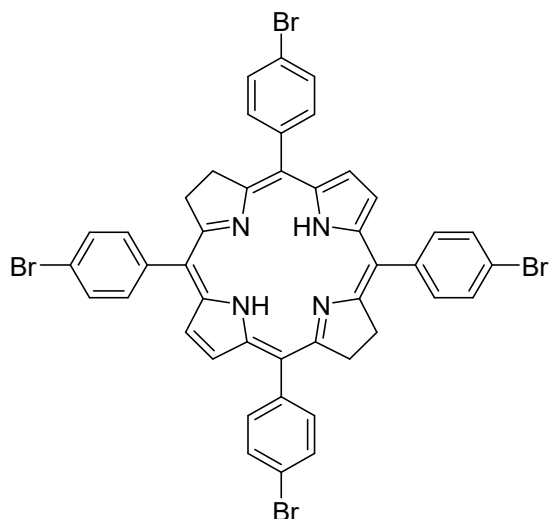
5,10,15,20-tetrakis(4-bromo-2,3,5,6-tetrafluorophenyl)-porphyrin (**5**). Purple solid; ¹H NMR (400 MHz, CDCl₃) δ 8.94 (s, 8H), -2.90 (s, 2H).



5,10,15,20-tetra(4-bromo-3,5-dimethoxyphenyl)-porphyrin (**6**). Violet-red solid; ^1H NMR (400 MHz, DMSO) δ 8.98 (s, 8H), 7.58 (s, 8H), 3.95 (s, 24H), -2.95 (s, 2H).



5,10,15,20-tetrakis(10-bromoanthracen-9-yl)-porphyrin (**7**).⁴ Violet solid; ^1H NMR (400 MHz, CDCl_3) δ 8.78 (d, $J = 8.9$ Hz, 8H), 8.10 (s, 8H), 7.59 – 7.51 (m, 8H), 7.19 (dd, $J = 8.9$, 4.3 Hz, 8H), 7.08 – 7.03 (m, 8H), -1.72 (s, 2H).



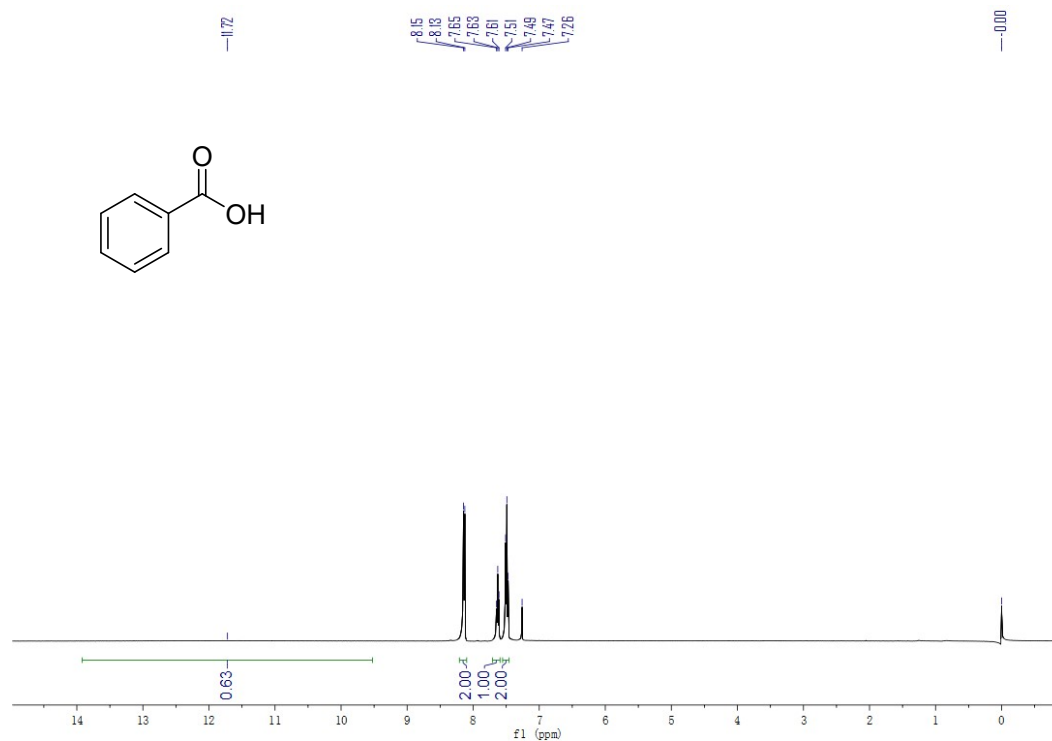
7,8,17,18-tetrahydro-5,10,15,20-tetrakis(4-bromophenyl)-21H,23H-porphine (**8**). Black solid; ^1H NMR (400 MHz, CDCl_3) δ 8.56 (d, $J = 4.8$ Hz, 2H), 8.19 (d, $J = 4.6$ Hz, 2H), 7.82 (d, $J = 8.0$ Hz, 8H), 7.73 (d, $J = 8.0$ Hz, 8H), 4.15 (s, 8H), -1.52 (s, 2H). ^{13}C NMR (101 MHz, CDCl_3) δ 167.29, 152.25, 141.71, 140.79, 140.54, 135.19, 133.80, 132.03, 131.36, 131.14, 129.98, 128.09, 123.50, 122.42, 122.04, 121.48, 111.18, 35.83, 29.71. HRMS (ESI-TOF, m/z): $[\text{M}+\text{Na}]^+$ calcd for $\text{C}_{44}\text{H}_{30}\text{N}_4\text{Br}_4\text{Na}$, 952.9102; found, 952.9088.

15. References

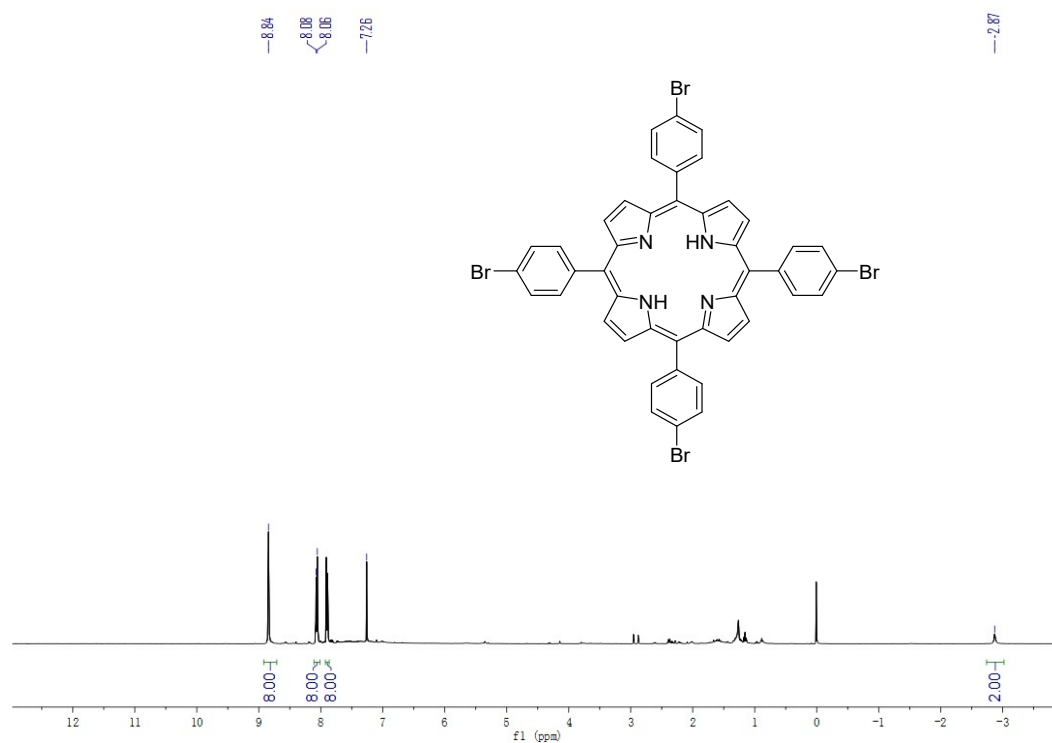
- S1. X. Sun, N. Zheng, G. Liu, Q. Wu and W. Song, *Chem. Commun.*, 2022, **58**, 13234-13237.
- S2. H. Ma, X. Xu, Y. Zheng and W. Song, *Fine Chemicals*, 2021, **38**.
- S3. A. Dong, D. Wang, T. Dai, Q. Chen, L. Feng and N. Wang, *Adv. Compos. Hybrid Mater.*, 2018, **1**, 696-704.
- S4. J. Pijeat, Y. J. Dappe, P. Thuéry and S. Campidelli, *Org. Biomol. Chem.*, 2018, **16**, 8106-8114.
- S5. H. Cao, G. Wang, Y. Xue, G. Yang, J. Tian, F. Liu and W. Zhang, *ACS Macro Lett.*, 2019, **8**, 616-622.
- S6. G. Laudadio, Y. Deng, K. van der Wal, D. Ravelli, M. Nuño, M. Fagnoni, D. Guthrie, Y. Sun and T. Noël, *Science*, 2020, **369**, 92-96.
- S7. G. Liu, N. Zheng, X. Duan, X. Sun and W. Song, *Green Chem.*, 2023, **25**, 5035-5040.
- S8. J. P. Phelan, S. B. Lang, J. Sim, S. Berritt, A. J. Peat, K. Billings, L. Fan and G. A. Molander, *J. Am. Chem. Soc.*, 2019, **141**, 3723-3732.
- S9. H. Liu, L. Zhao, Y. Yuan, Z. Xu, K. Chen, S. Qiu and H. Tan, *Acs Catal.*, 2016, **6**, 1732-1736.
- S10. S. Mukherjee, B. Maji, A. Tlahuext-Aca and F. Glorius, *J. Am. Chem. Soc.*, 2016, **138**, 16200-16203.
- S11. S. Liu, J. Ma, E. Y. Xue, S. Wang, Y. Zheng, D. K. P. Ng, A. Wang and N. Zheng, *Adv. Healthcare Mater.*, 2023, **12**, 2300481.
- S12. J. Bai, X. Xu, Y. Zheng, W. Song and N. Zheng, *Green. Synth. Catal.*, 2023, DOI: 10.1016/j.gresc.2023.03.001.
- S13. Y. Qin, T. Zhang, H. Y. V. Ching, G. S. Raman and S. Das, *Chem*, 2022, **8**, 2472-2484.
- S14. Z. Huang, M. Shanmugam, Z. Liu, A. Brookfield, E. L. Bennett, R. Guan, D. E. Vega Herrera, J. A. Lopez-Sanchez, A. G. Slater, E. J. L. McInnes, X. Qi and J. Xiao, *J. Am. Chem. Soc.*, 2022, **144**, 6532-6542.

16. Copies of NMR Spectra of Products

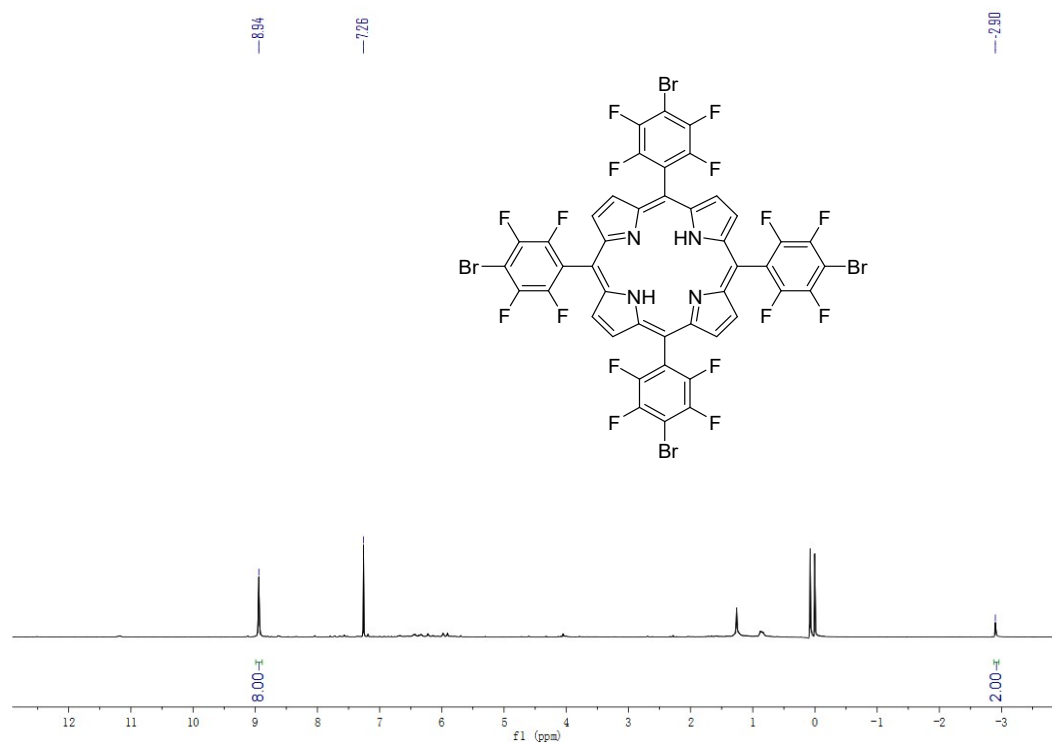
^1H NMR (400 MHz, CDCl_3) of benzoic acid



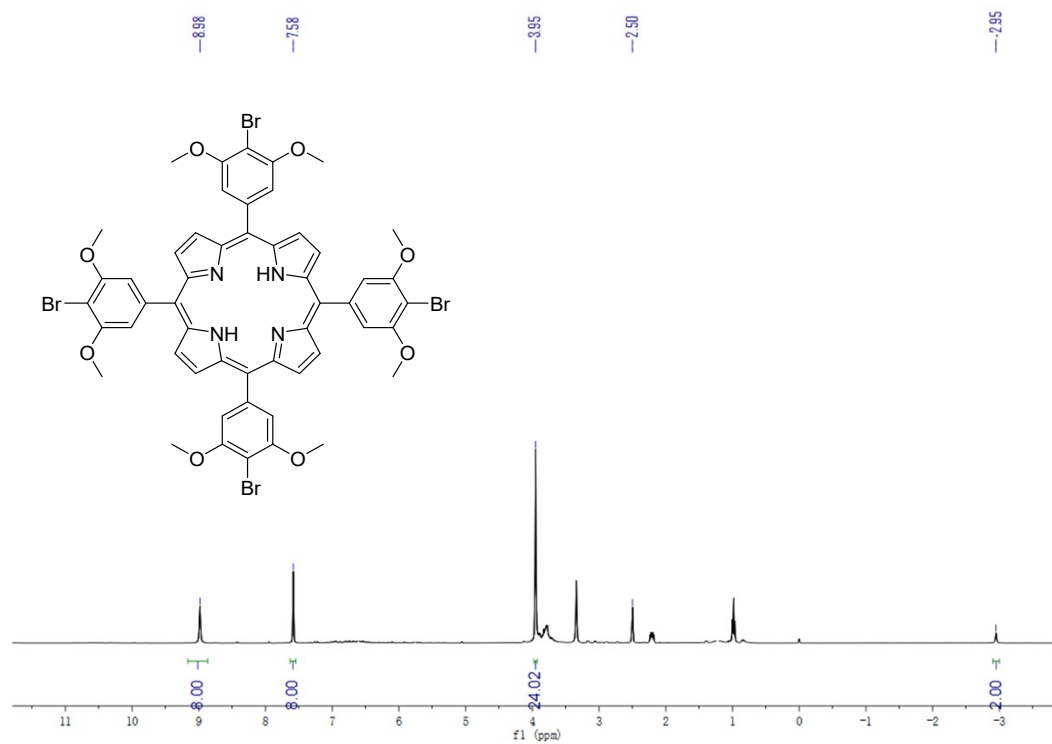
^1H NMR (400 MHz, CDCl_3) of 5,10,15,20-tetrakis(4-bromophenyl)-porphyrin (**1**)



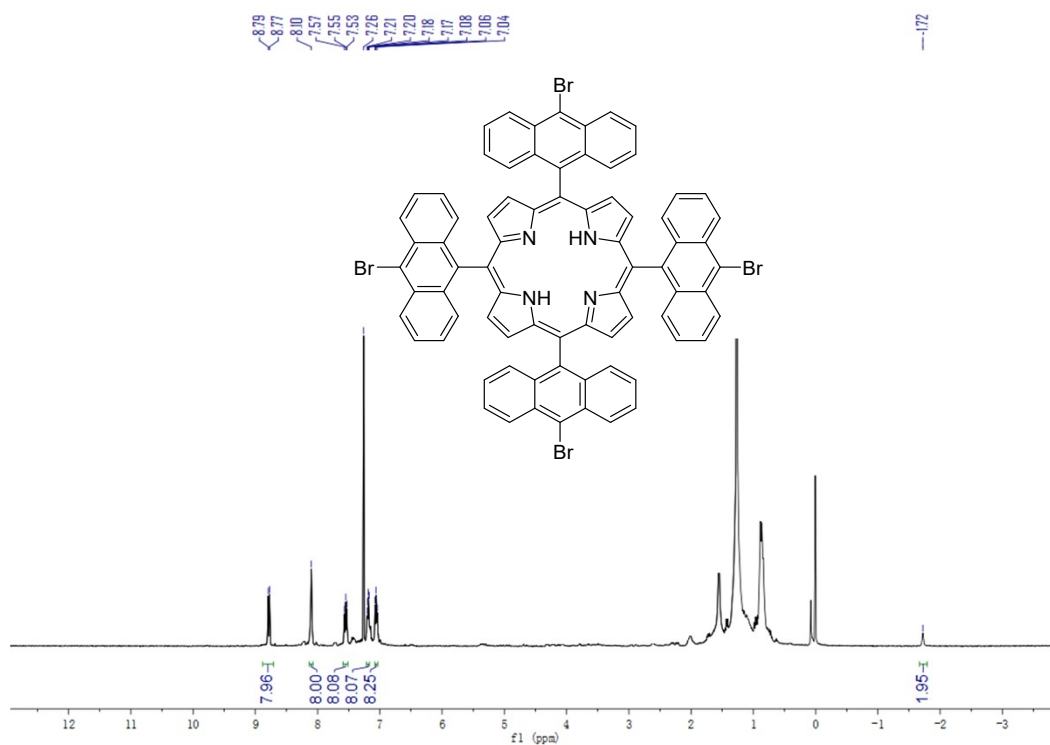
^1H NMR (400 MHz, CDCl_3) of 5,10,15,20-tetrakis(4-bromo-2,3,5,6-tetrafluorophenyl)-porphyrin (**5**)



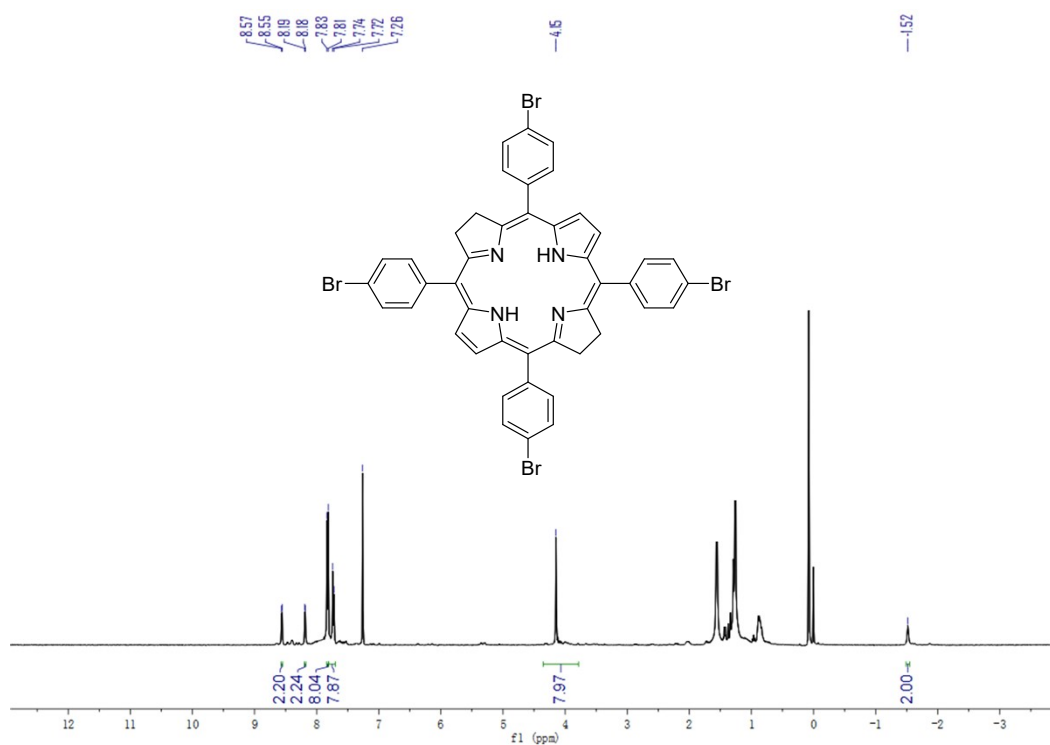
^1H NMR (400 MHz, DMSO) of 5,10,15,20-tetra(4-bromo-3,5-dimethoxyphenyl)-porphyrin (**6**)



^1H NMR (400 MHz, CDCl_3) of 5,10,15,20-tetrakis(10-bromoanthracen-9-yl)-porphyrin (**7**)



^1H NMR (400 MHz, CDCl_3) of 7,8,17,18-tetrahydro-5,10,15,20-tetrakis(4-bromophenyl)-21H,23H-porphine (**8**)



^{13}C NMR (101 MHz, CDCl_3) of 7,8,17,18-tetrahydro-5,10,15,20-tetrakis(4-bromophenyl)-21H,23H-porphine (**8**)

